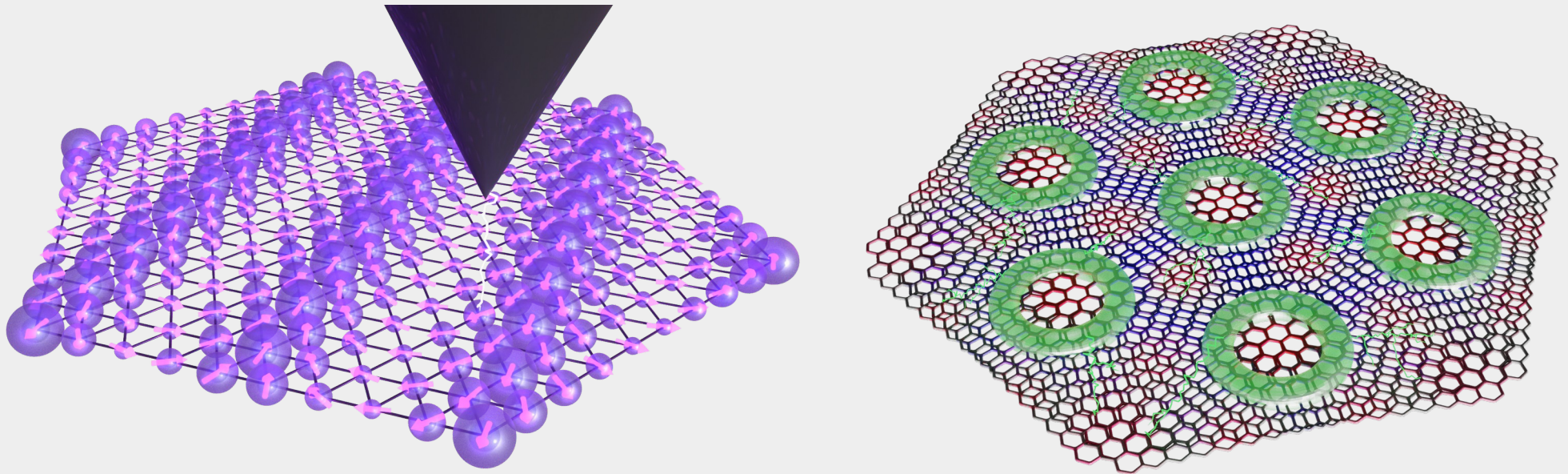


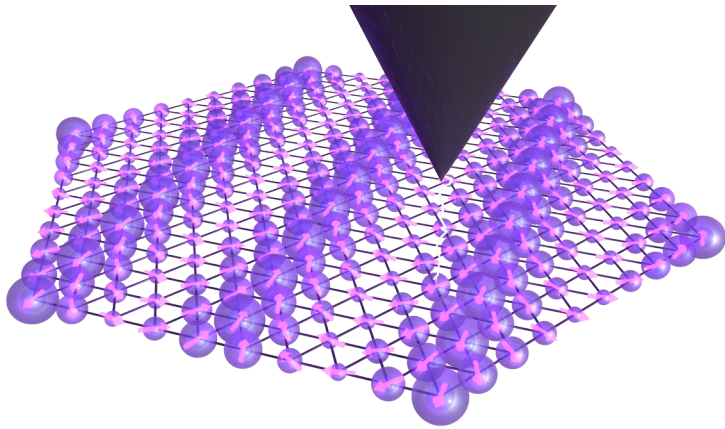
Multiferroic van der Waals Materials



Adolfo O Fumega

Researchers

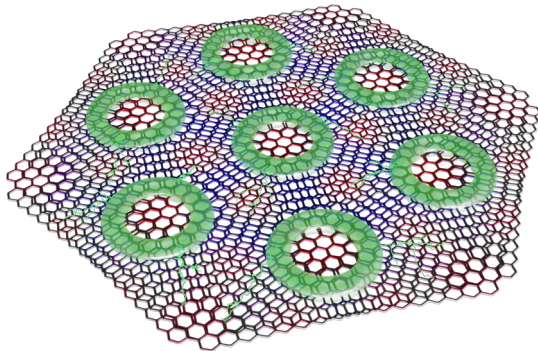
The first 2D Multiferroic



Adolfo O. Fumega and Jose L. Lado
2D Materials 9, 025010 (2022)

Mohammad Amini,* **Adolfo O Fumega**,*
Héctor González-Herrero,
Viliam Vaňo, Shawulienu Kezilebieke,
Jose L Lado⁺, Peter Liljeroth⁺
Advanced Materials 2311342 (2024)

Artificial Moiré Multiferroics



Adolfo O. Fumega and Jose L. Lado
2D Materials 10, 025026 (2023)

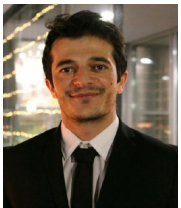
Researchers

Adolfo O. Fumega and Jose L. Lado
[2D Materials 9, 025010 \(2022\)](#)

Mohammad Amini,* **Adolfo O Fumega**,* Héctor González-Herrero,
Viliam Vaňo, Shawulienu Kezilebieke, Jose L Lado⁺, Peter Liljeroth⁺
[Advanced Materials 2311342 \(2024\)](#)

Adolfo O. Fumega and Jose L. Lado
[2D Materials 10, 025026 \(2023\)](#)

Aalto University



Mohammad
Amini



Jose L
Lado



Peter
Liljeroth

Princeton University



Viliam
Vaňo

Autonomous University of Madrid



Héctor
González
Herrero

University of Jyväskylä



Shawulienu
Kezilebieke

Motivation

Multiferroics



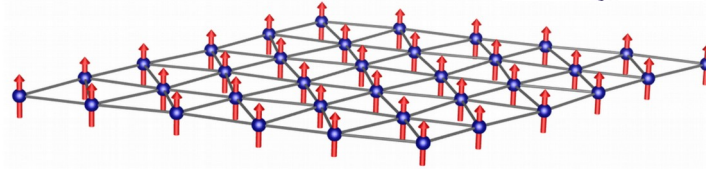
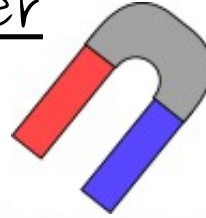
Materials with
more than one
Ferroic order

Motivation

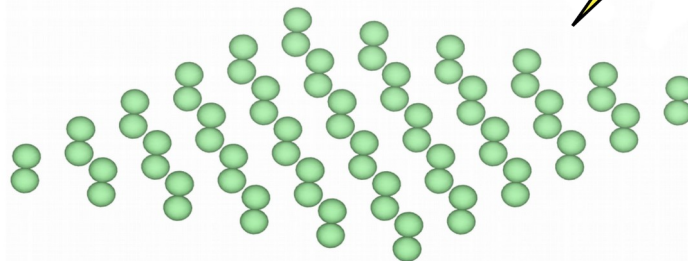
Multiferroics

Materials with
more than one
Ferroic order

Magnetic order



Electric order

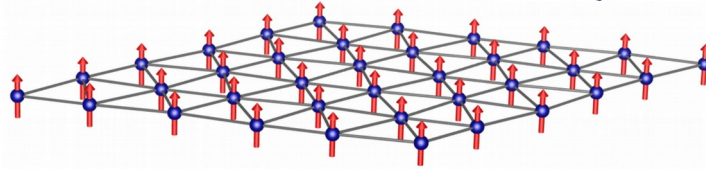
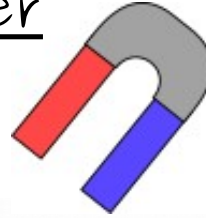


Motivation

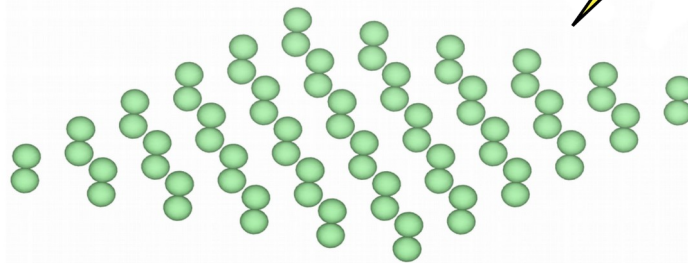
Multiferroics

Materials with
more than one
Ferroic order

Magnetic order



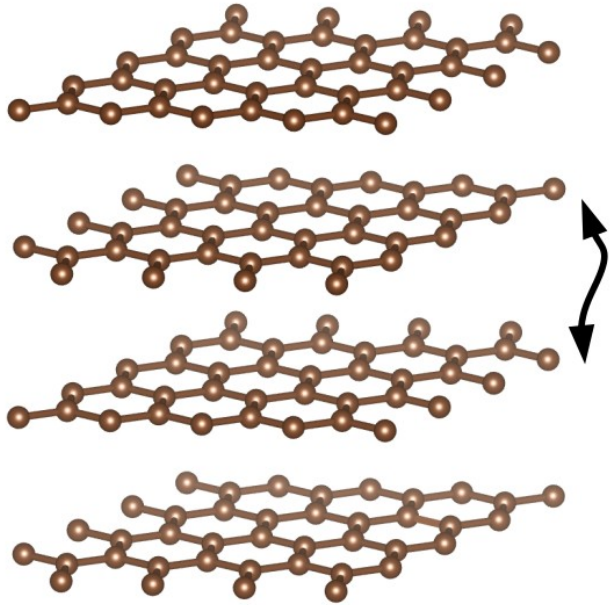
Electric order



Magnetolectric
Coupling

Motivation

Layered van der Waals

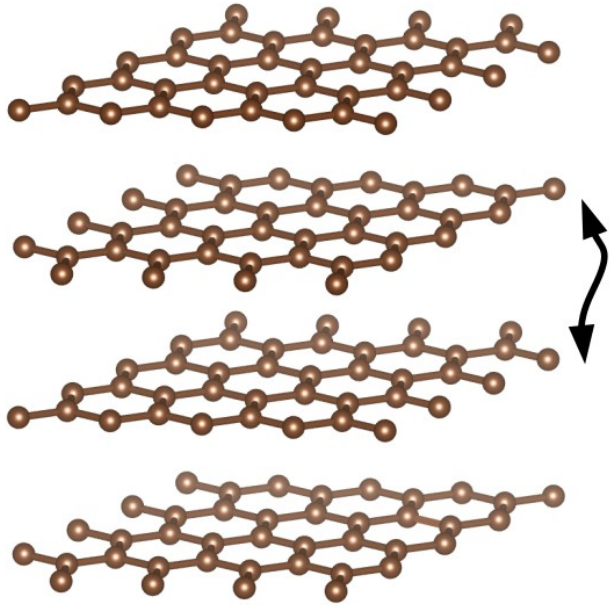


Graphite

Weak
van der Waals
bonding

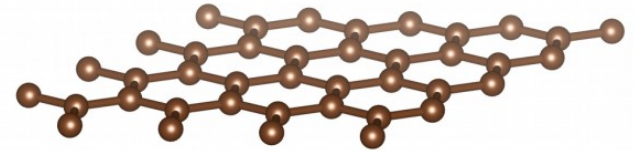
Motivation

Layered van der Waals



Graphite

Weak
van der Waals
bonding



Graphene

Reach the
2D limit !!!

Motivation

Layered van der Waals

Monolayer

Semimetal

Graphene

Insulator

BN

Superconductor

NbSe₂

Ferromagnet

CrI₃

Ferroelectric

MoTe₂

Multiferroic

NiI₂

...

Motivation

Layered van der Waals

Monolayer

Semimetal

Graphene

Insulator

BN

Superconductor

NbSe₂

Ferromagnet

CrI₃

Ferroelectric

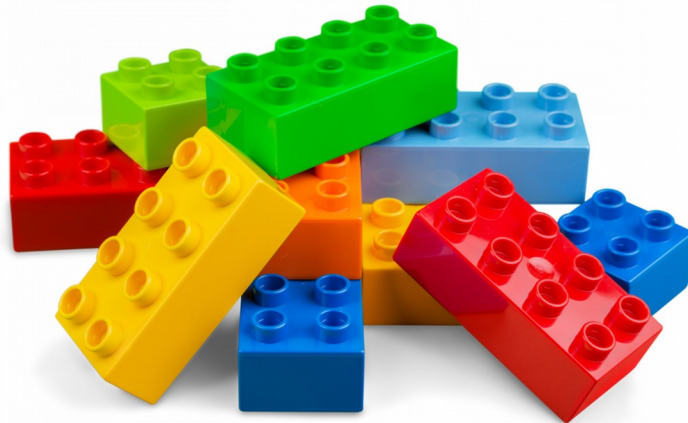
MoTe₂

Multiferroic

NiI₂

...

2D building blocks



Motivation

Layered van der Waals

Monolayer

Semimetal

Insulator

Superconductor

Ferromagnet

Ferroelectric

Multiferroic ...

Graphene

BN

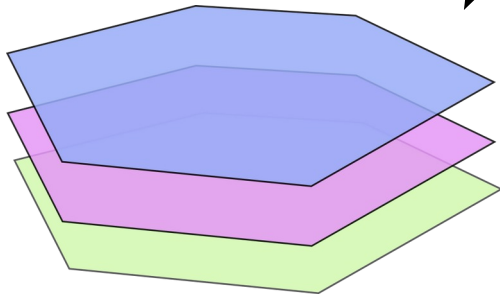
NbSe₂

CrI₃

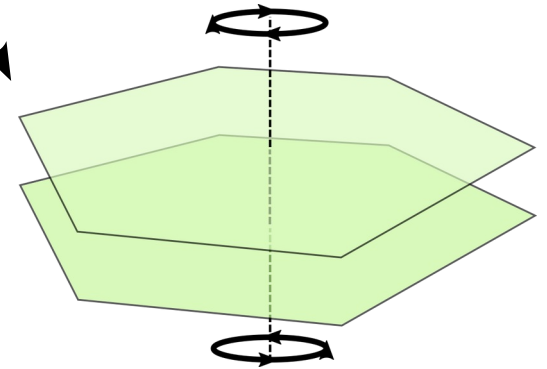
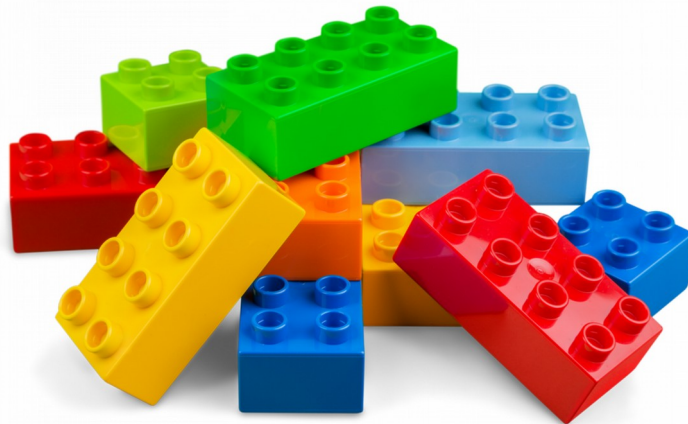
MoTe₂

NiI₂

2D building blocks



Heterostructures



Twisted layers

Motivation

Layered van der Waals

Monolayer

Semimetal

Graphene

Insulator

BN

Superconductor

NbSe₂

Ferromagnet

CrI₃

Ferroelectric

MoTe₂

Multiferroic

NiI₂

...

The first 2D Multiferroic

Evidence for a single-layer van der Waals multiferroic
Song et al., [Nature 602, 601-605 \(2022\)](#)

Motivation

Layered van der Waals

Monolayer

Semimetal

Graphene

Insulator

BN

Superconductor

NbSe₂

Ferromagnet

CrI₃

Ferroelectric

MoTe₂

Multiferroic

NiI₂

...

The first 2D Multiferroic

Evidence for a single-layer van der Waals multiferroic
Song et al., [Nature 602, 601-605 \(2022\)](#)

Experimental evidence
optical techniques



Motivation

Layered van der Waals

Monolayer

Semimetal

Graphene

Insulator

BN

Superconductor

NbSe₂

Ferromagnet

CrI₃

Ferroelectric

MoTe₂

Multiferroic

NiI₂

...

The first 2D Multiferroic

Evidence for a single-layer van der Waals multiferroic
Song et al., [Nature 602, 601-605 \(2022\)](#)

Experimental evidence
optical techniques

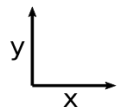
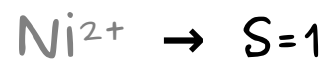
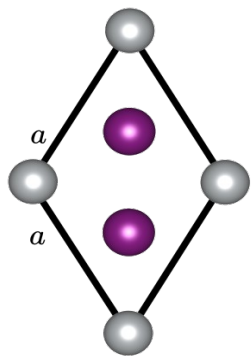


Origin of the multiferroic order in monolayer NiI₂!

New methods to prove and characterize 2D multiferroics!

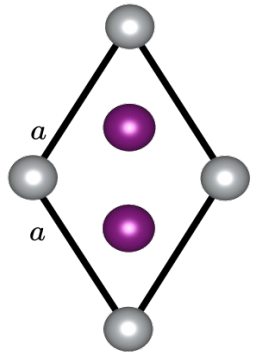
Multiferroicity in NiI_2

NiI_2

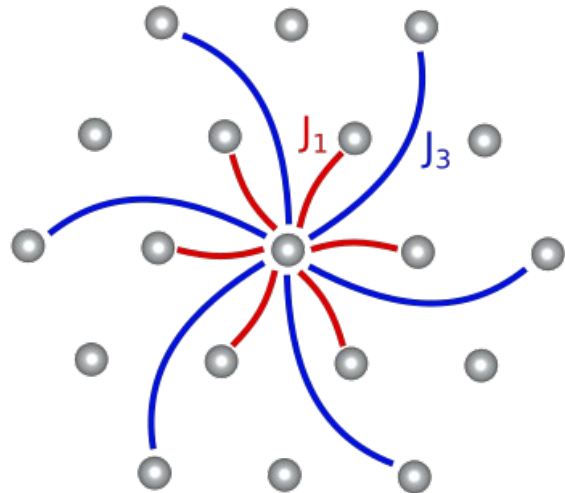
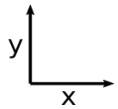


Multiferroicity in NiI_2

NiI_2



$\text{Ni}^{2+} \rightarrow S=1$



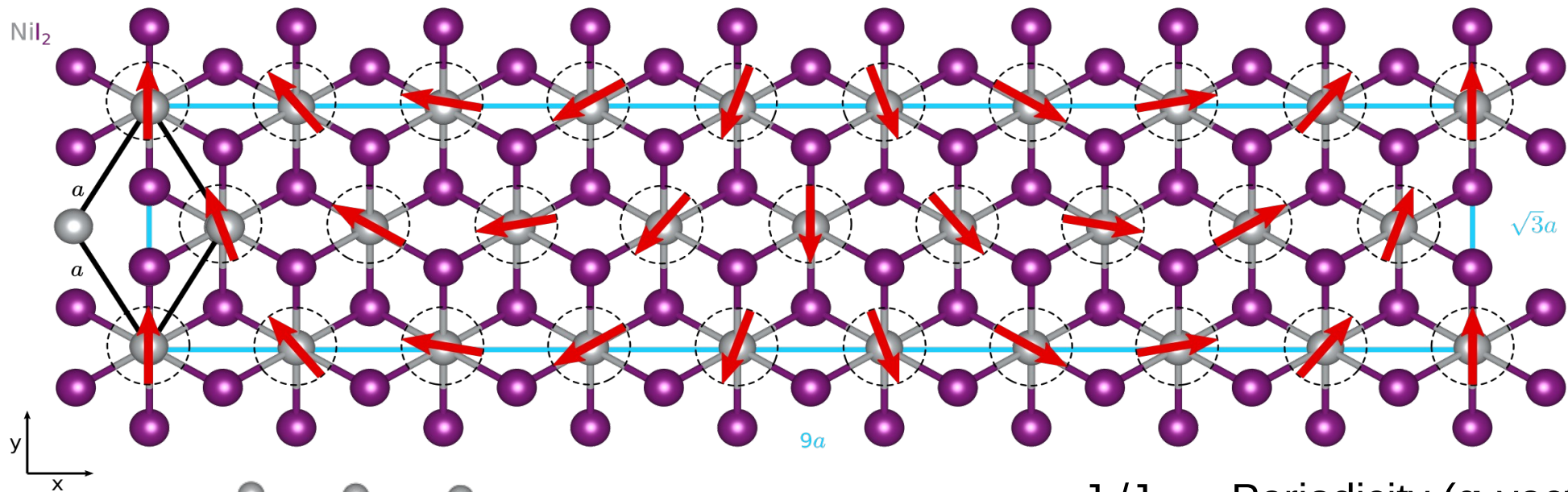
$J_1 \rightarrow$ Ferromagnetic exchange



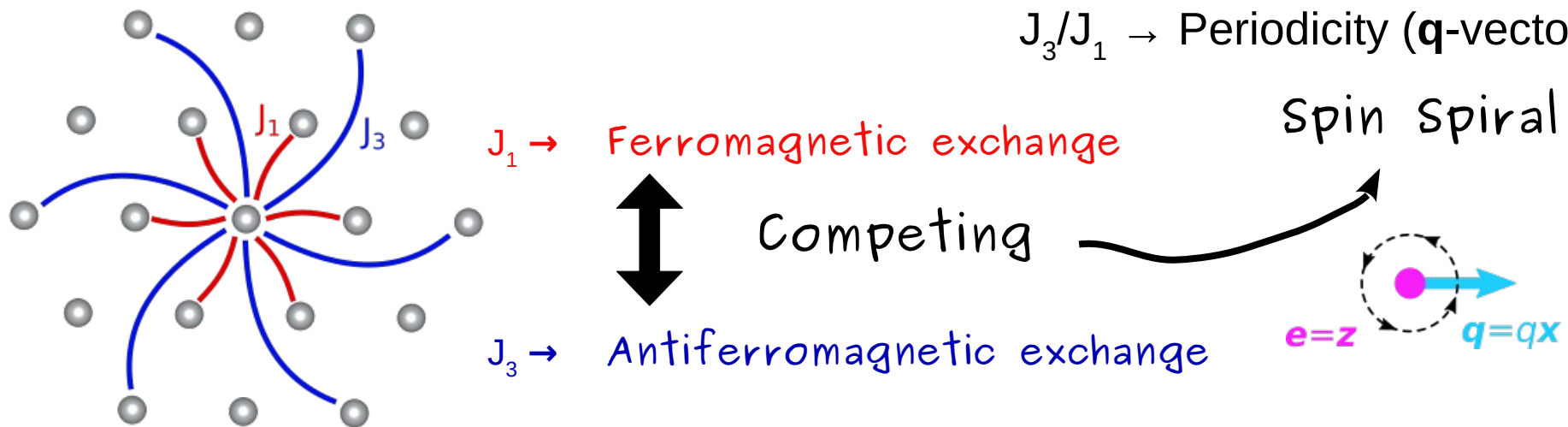
Competing

$J_3 \rightarrow$ Antiferromagnetic exchange

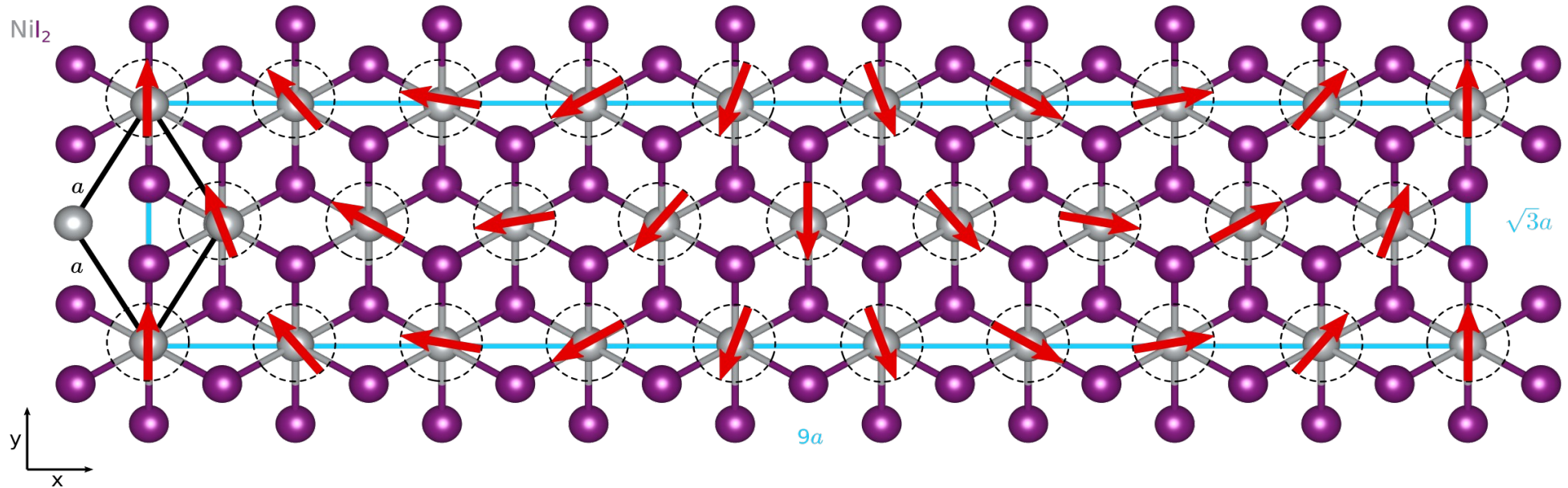
Multiferroicity in NiI_2



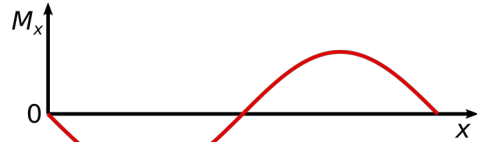
$J_3/J_1 \rightarrow$ Periodicity (q -vector)



Multiferroicity in NiI_2



Spiral Magnetization

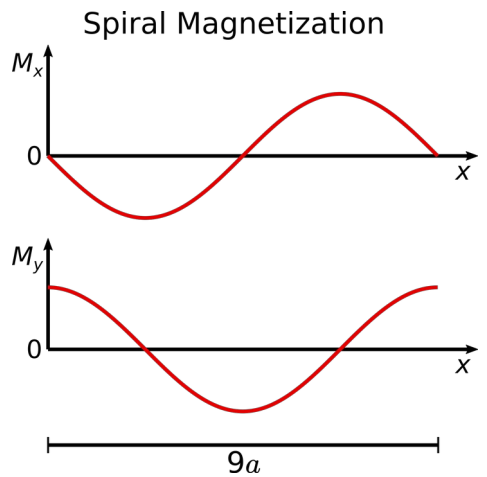
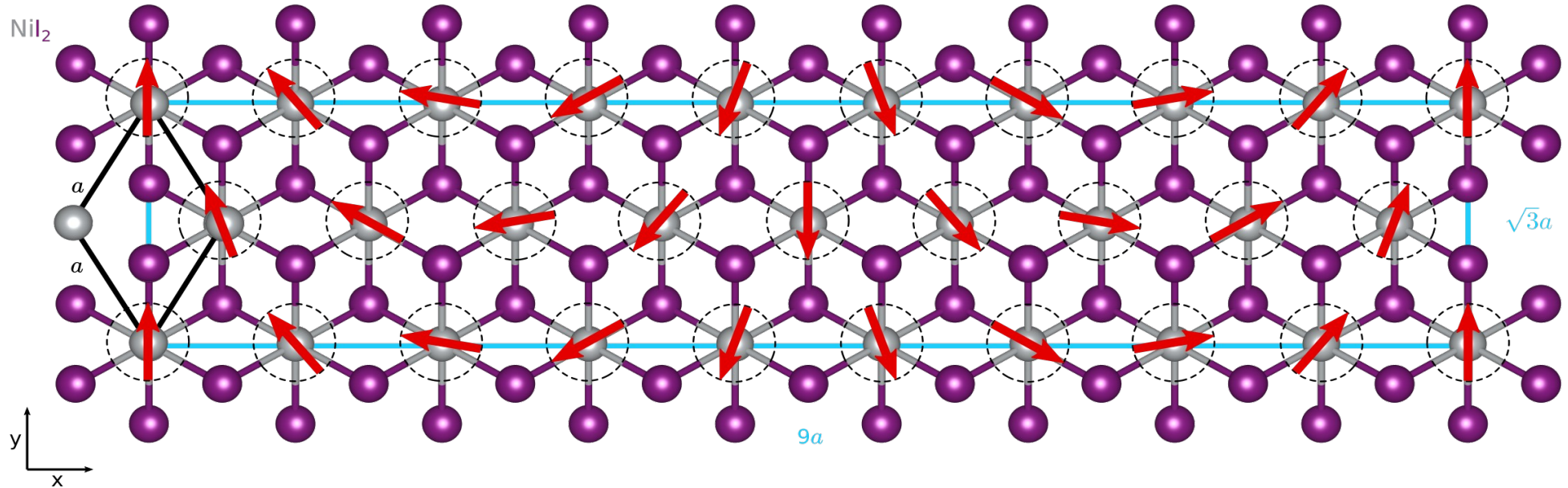


$$\mathbf{M} = M(-\sin(\mathbf{q}\mathbf{r}), \cos(\mathbf{q}\mathbf{r}), 0)$$



$9a$

Multiferroicity in NiI_2



$$\mathbf{M} = M(-\sin(\mathbf{q}\mathbf{r}), \cos(\mathbf{q}\mathbf{r}), 0)$$

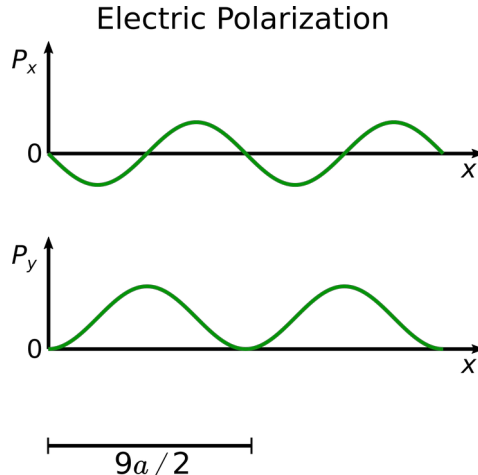
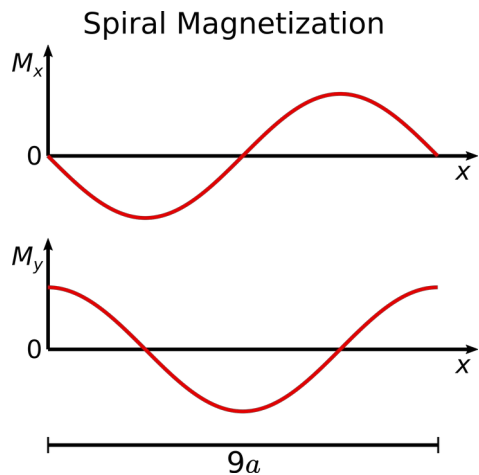
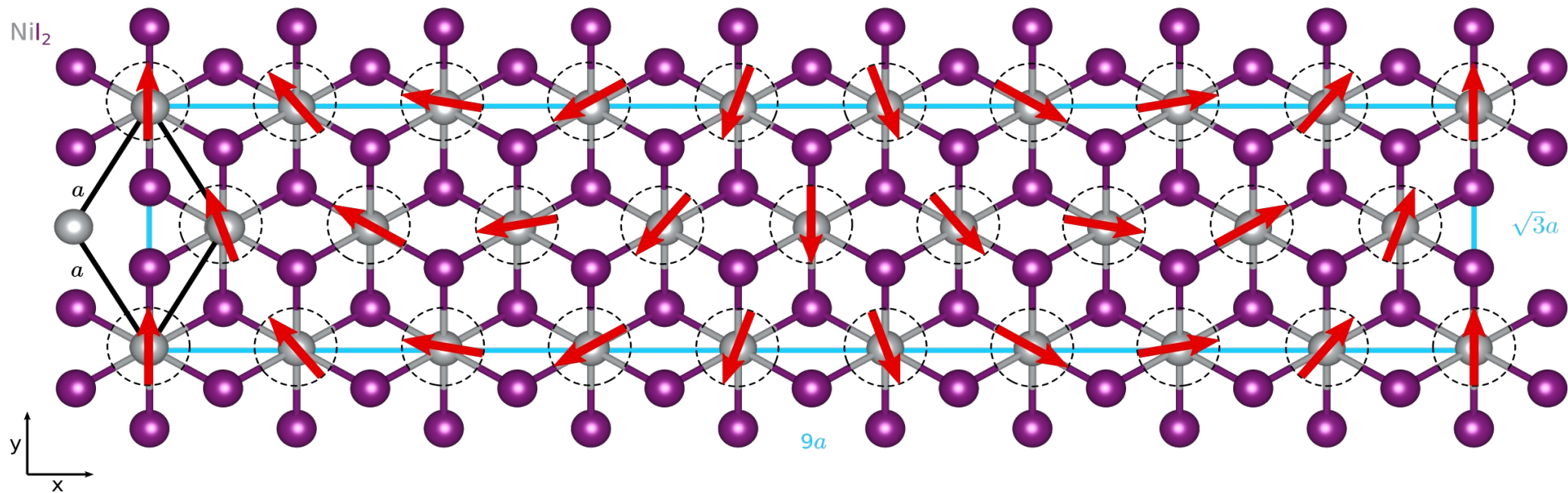
$$\mathbf{P} = \Lambda \frac{\mathbf{M} \times (\nabla \times \mathbf{M})}{M^2}$$

Spin-orbit coupling from I atoms

Mostovoy, *Phys. Rev. Lett.* 96, 067601 (2006)

AOF and Jose Lado, *2D Materials* 9 (2), 025010 (2022)

Multiferroicity in NiI_2

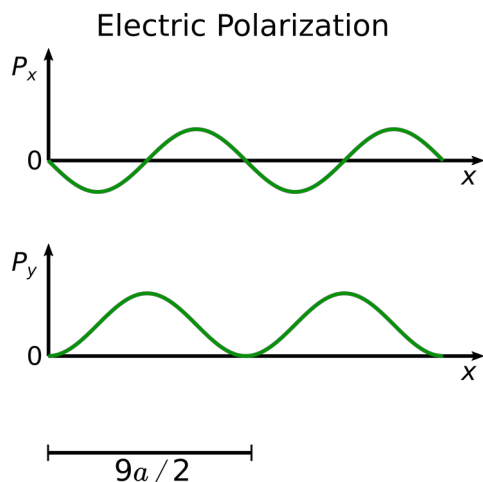
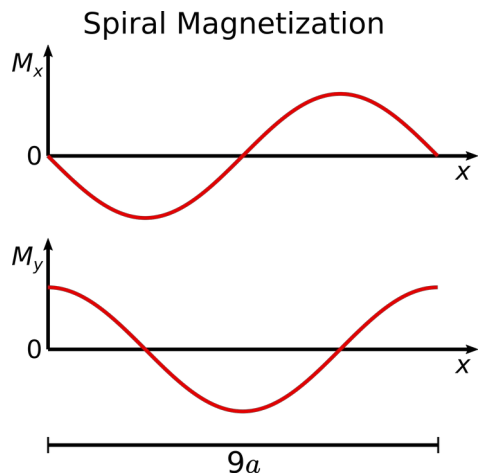
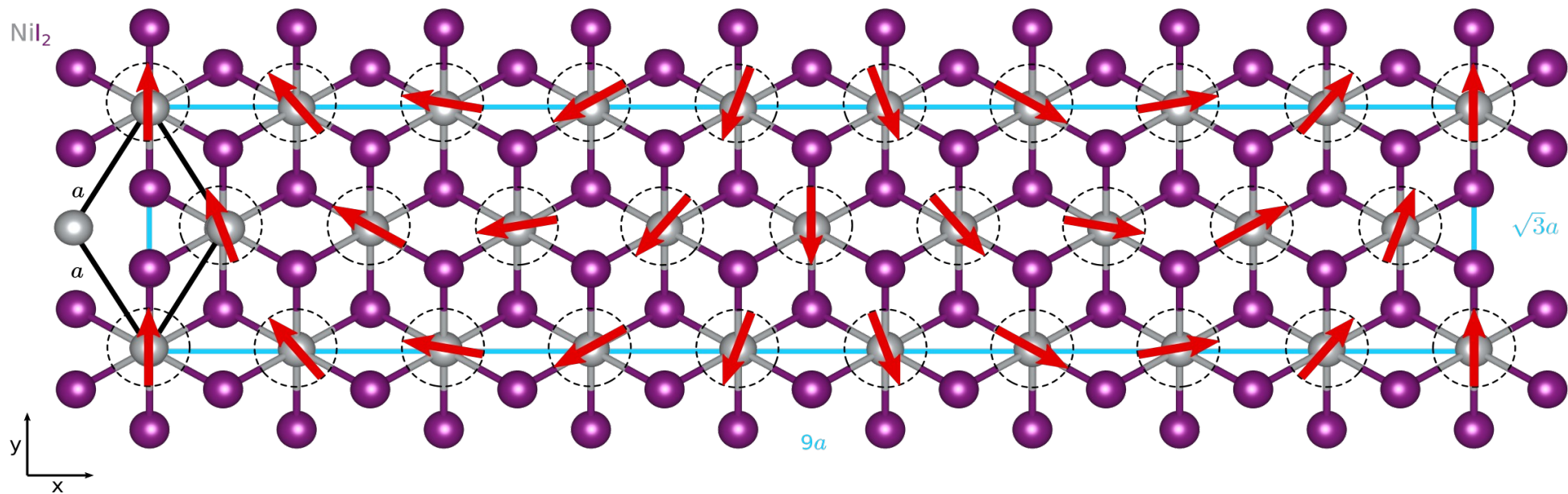


$$\mathbf{M} = M(-\sin(\mathbf{q}\mathbf{r}), \cos(\mathbf{q}\mathbf{r}), 0)$$

Half the periodicity

$$\mathbf{P} = \Lambda\mathbf{q}(-\sin(2\mathbf{q} \cdot \mathbf{r})/2, \sin^2(\mathbf{q} \cdot \mathbf{r}), 0)$$

Multiferroicity in NiI_2



Mostovoy, *Phys. Rev. Lett.* **96**, 067601 (2006)

$$\bar{\mathbf{P}} \propto \lambda_{\text{soc}}(\mathbf{e} \times \mathbf{q})$$

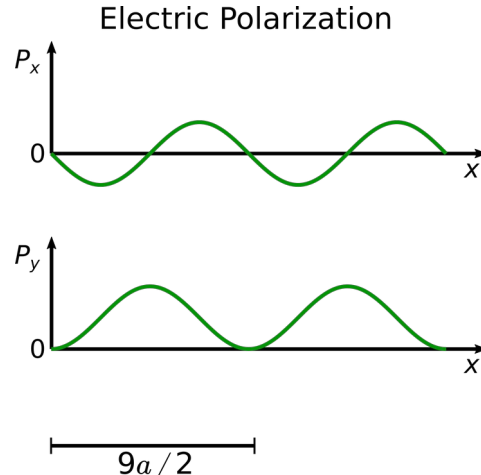
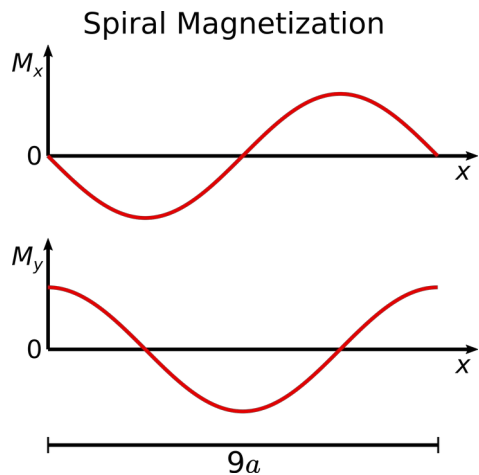
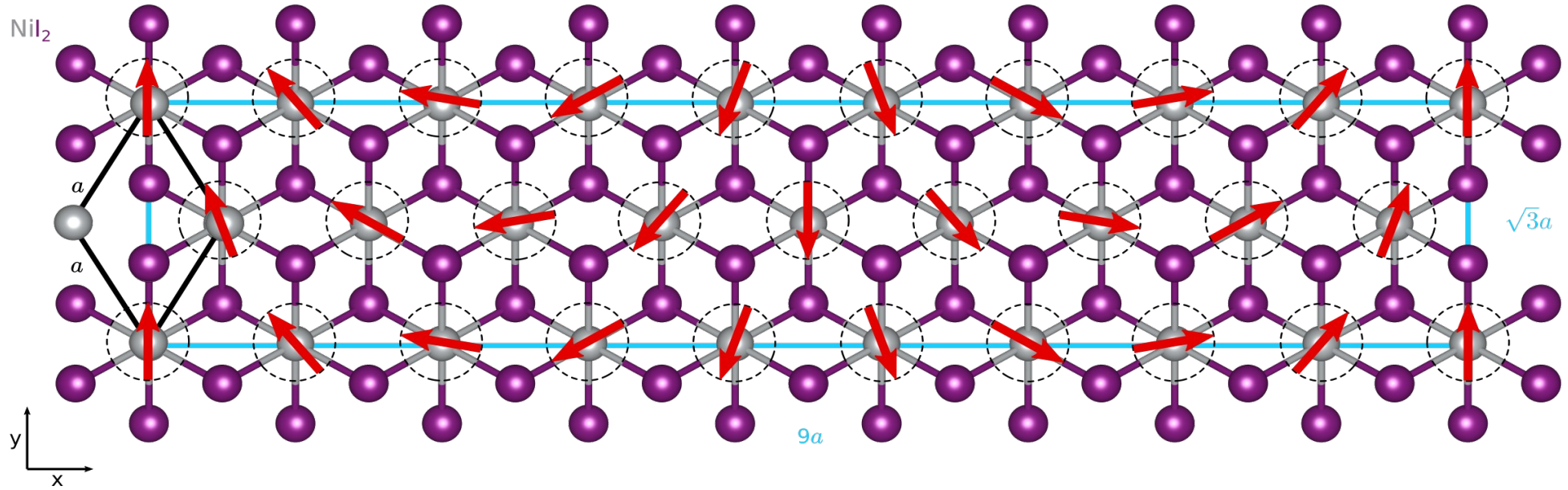
\bar{P}_y

$\mathbf{e} = z$

$\mathbf{q} = qx$

$$\mathbf{P} = \Lambda \mathbf{q} (-\sin(2\mathbf{q} \cdot \mathbf{r})/2, \sin^2(\mathbf{q} \cdot \mathbf{r}), 0)$$

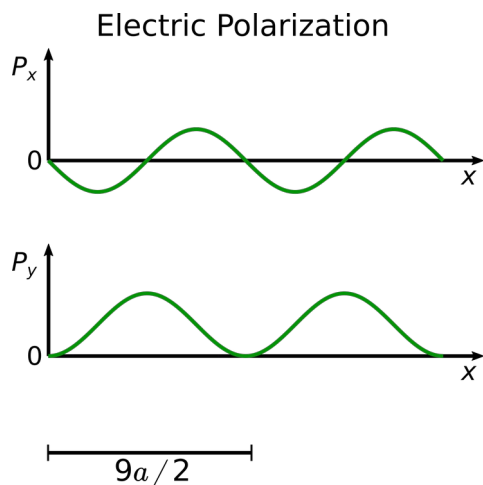
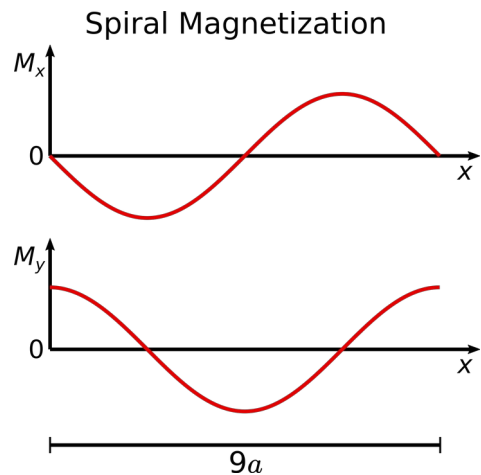
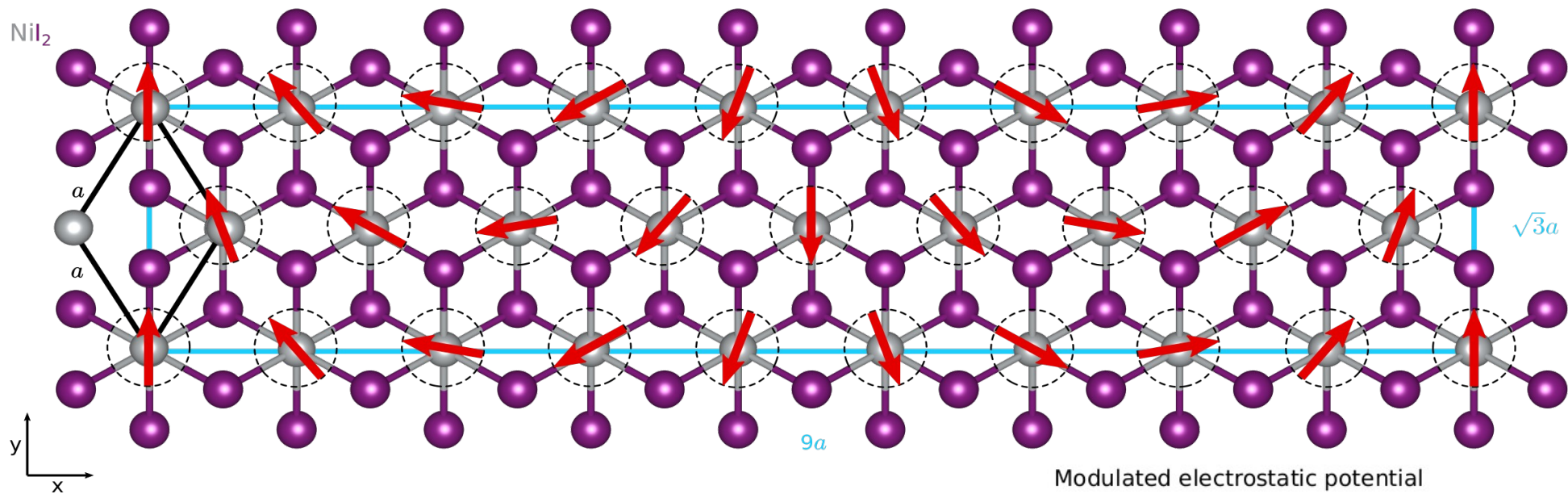
Multiferroicity in NiI_2



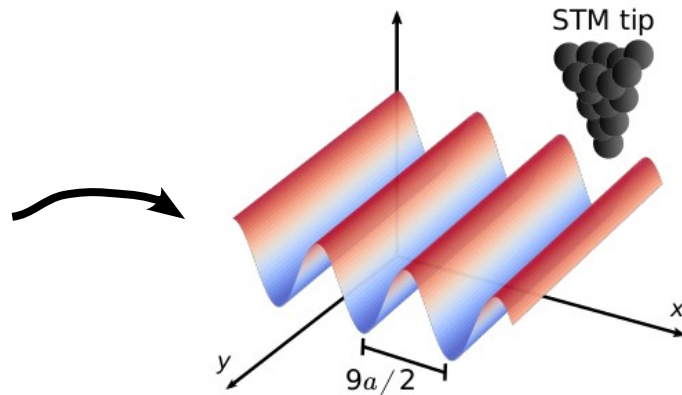
But at the atomic scale...

$$\mathbf{P} = \Lambda \mathbf{q} (-\sin(2\mathbf{q} \cdot \mathbf{r})/2, \sin^2(\mathbf{q} \cdot \mathbf{r}), 0)$$

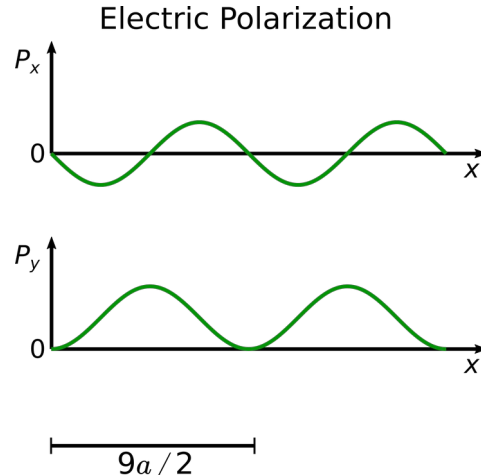
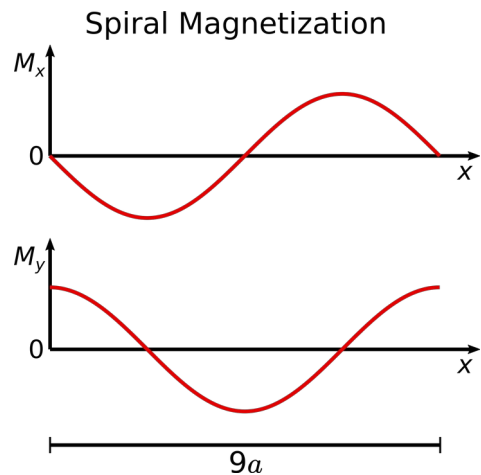
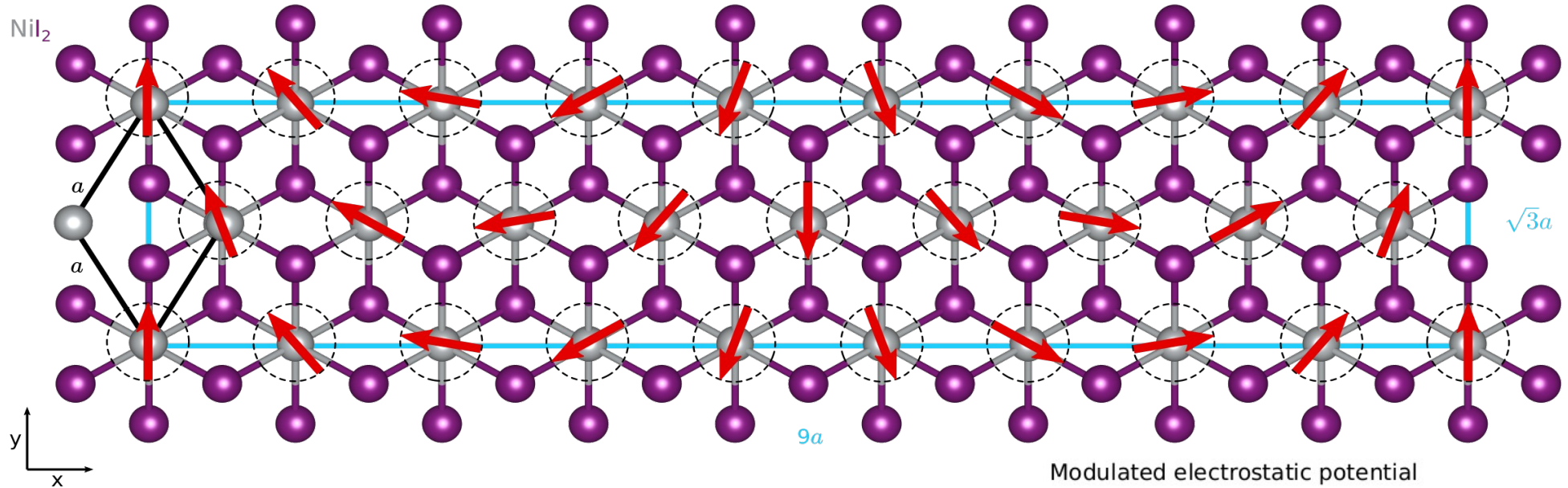
Multiferroicity in NiI_2



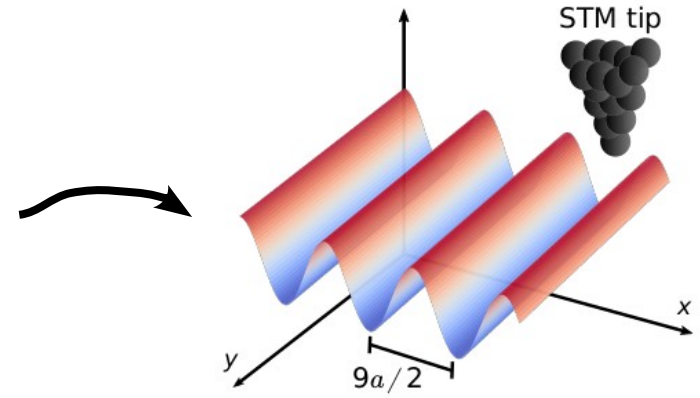
Modulated electrostatic potential



Multiferroicity in NiI_2

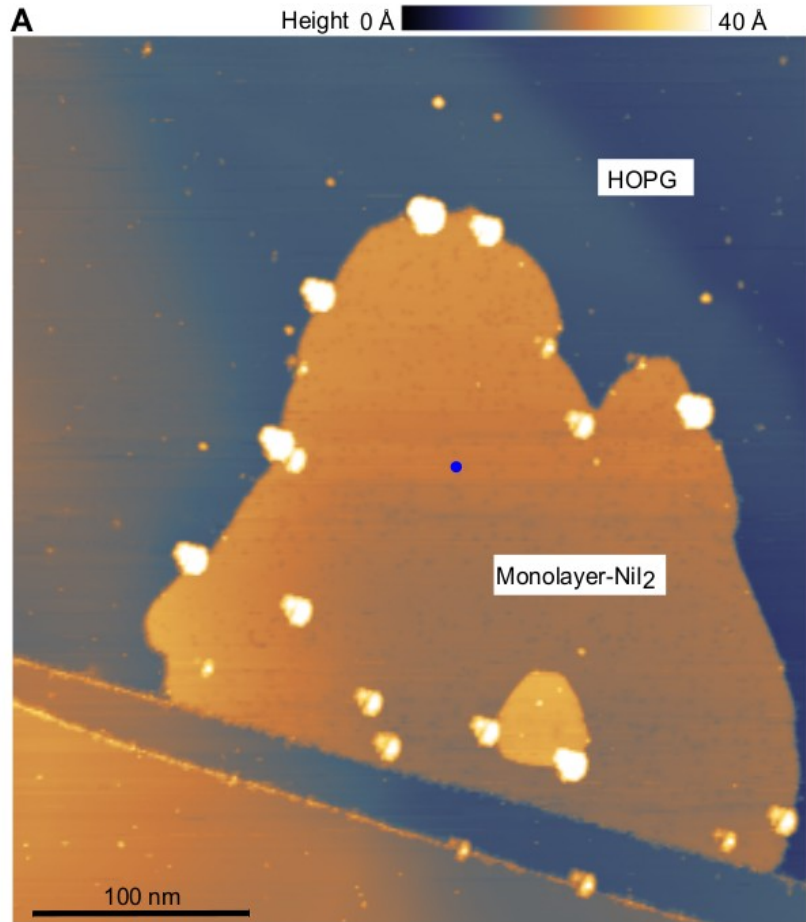


Modulated electrostatic potential



No need of spin-polarized techniques!

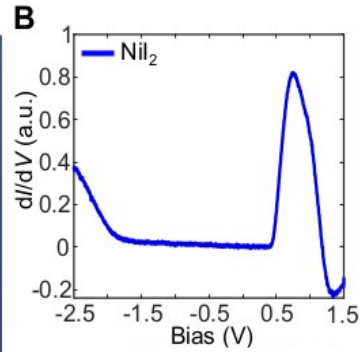
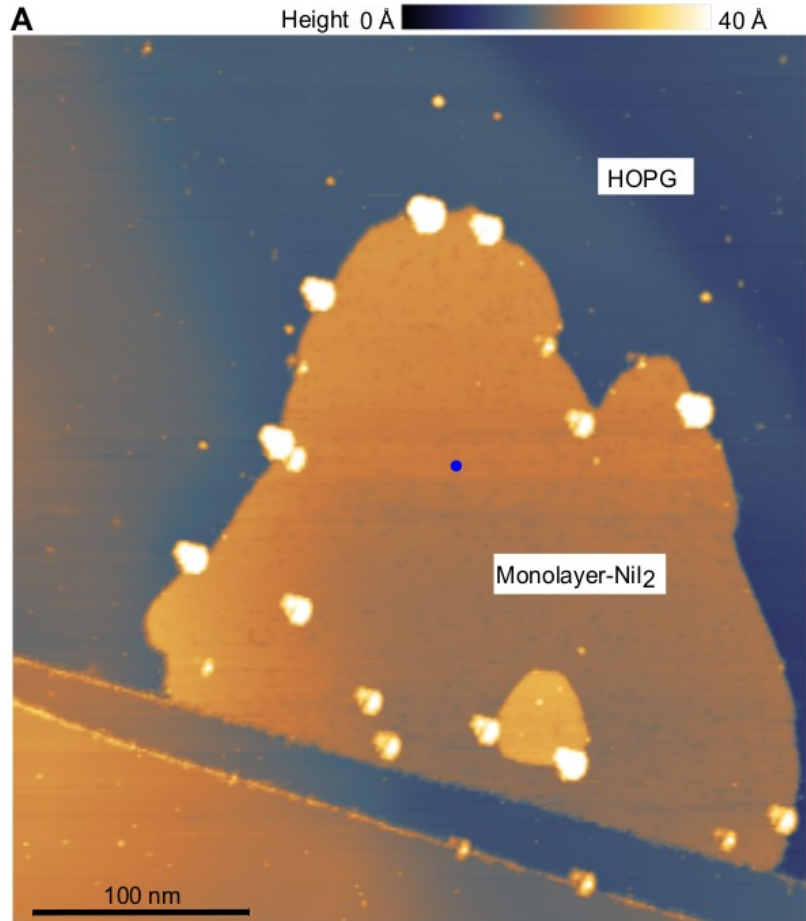
STM characterization of monolayer NiI_2



Monolayer NiI_2 on top of
Highly-oriented pyrolytic Graphite
(HOPG)

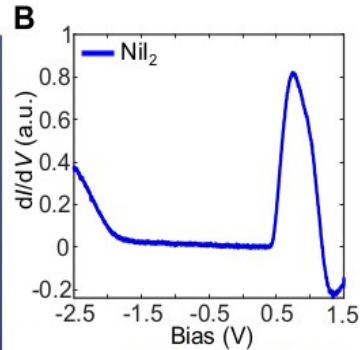
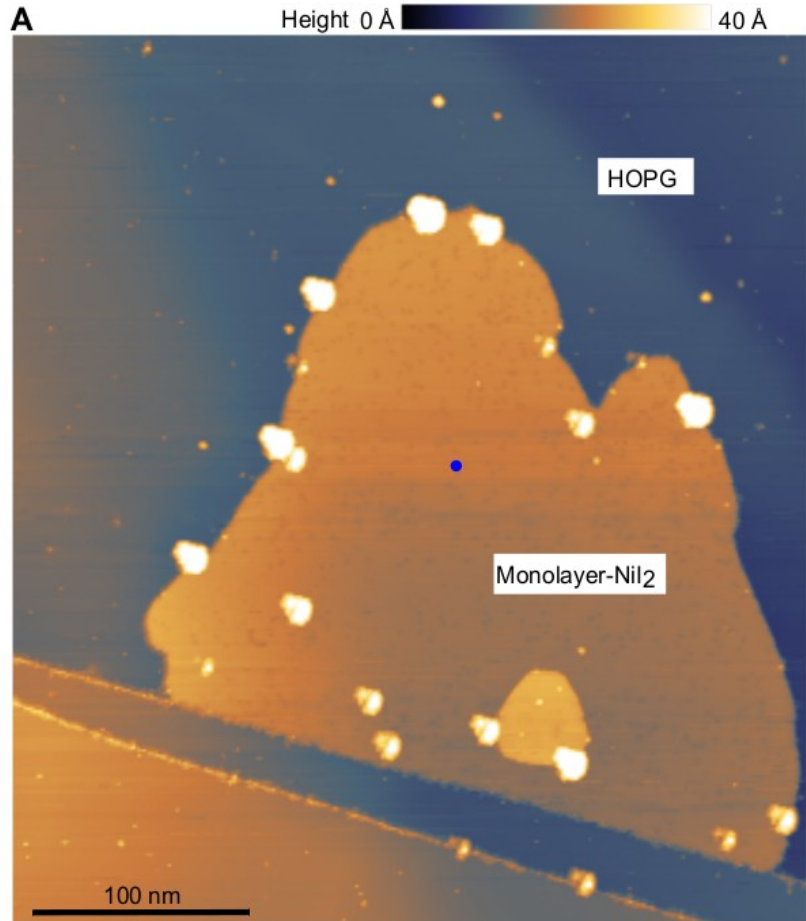


STM characterization of monolayer NiI_2

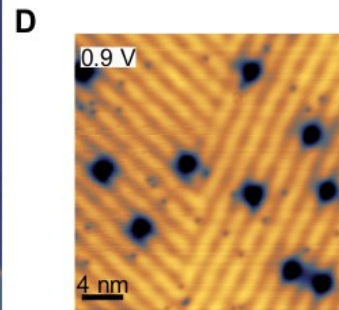


Monolayer NiI_2 is an insulator with a gap of 2.3 eV (from -1.9 to 0.4 V)

STM characterization of monolayer NiI_2



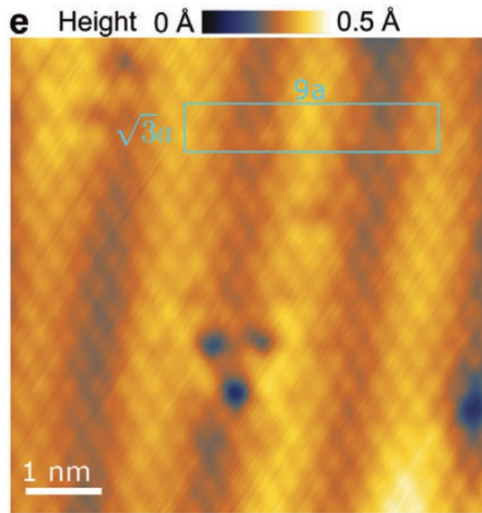
Monolayer NiI_2 is an insulator with a gap of 2.3 eV (from -1.9 to 0.4 V)



Scan within the conduction band of NiI_2
→
Stripy modulation

Demonstration of multiferroicity!

STM characterization of monolayer NiI_2

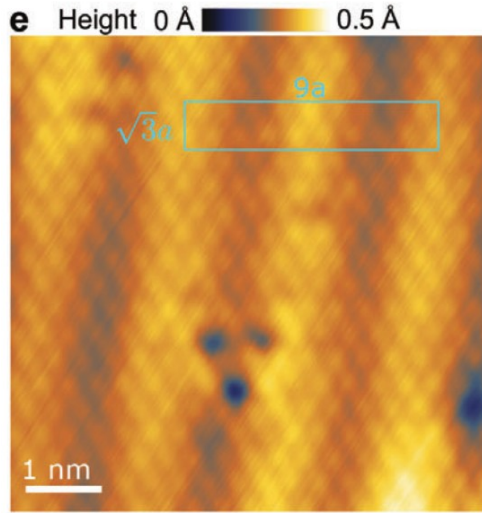


Experiment

Atomic resolution STM scan

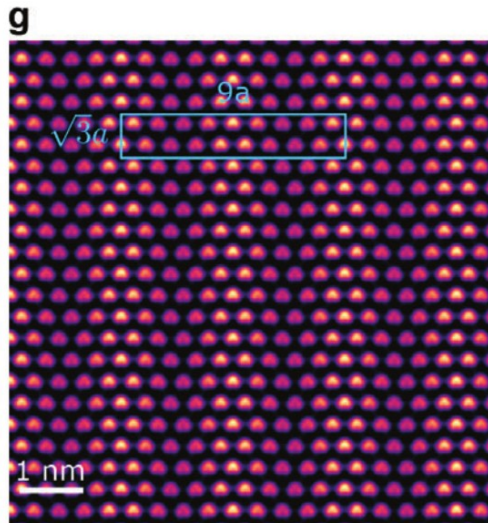
STM characterization of monolayer NiI_2

Experiment

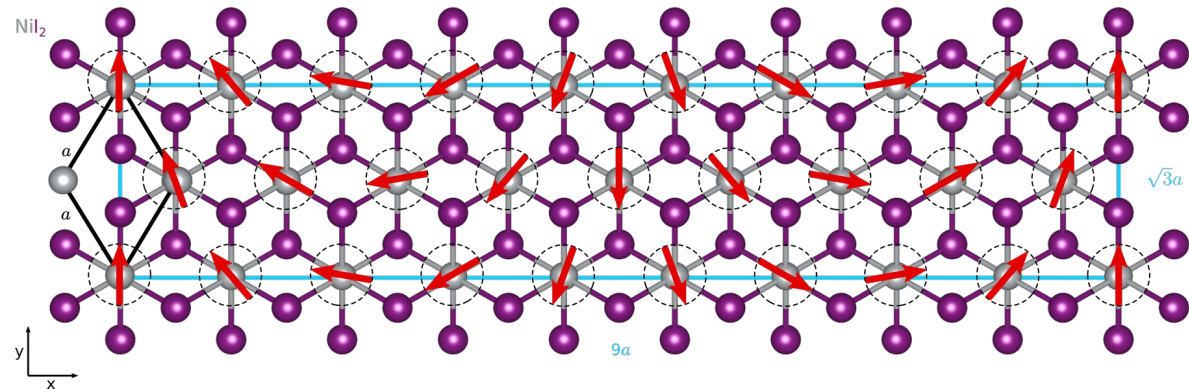


Atomic resolution STM scan

Theory

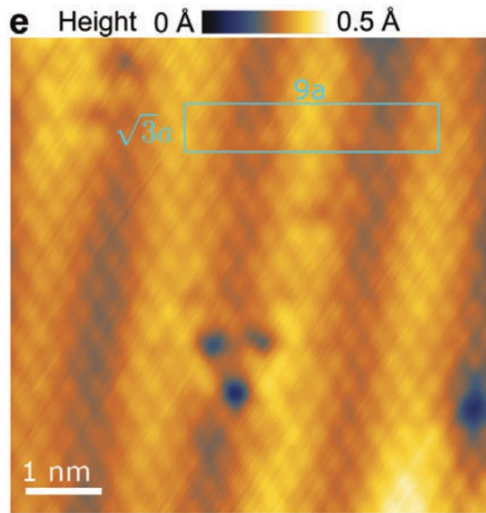


Commensurate supercell $9a \times \sqrt{3}a$

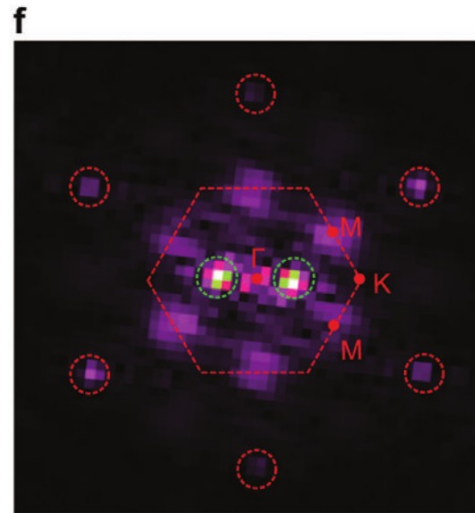


STM characterization of monolayer NiI_2

Experiment

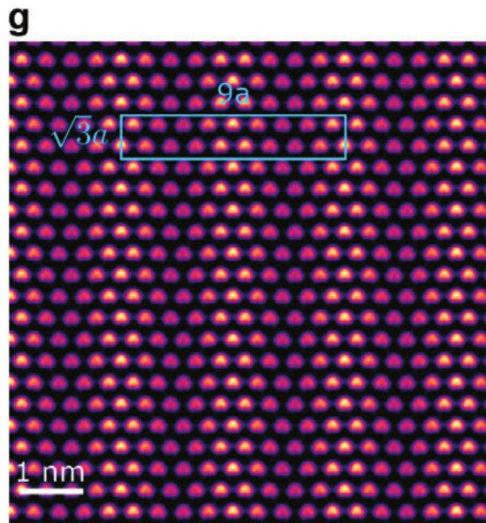


FFT

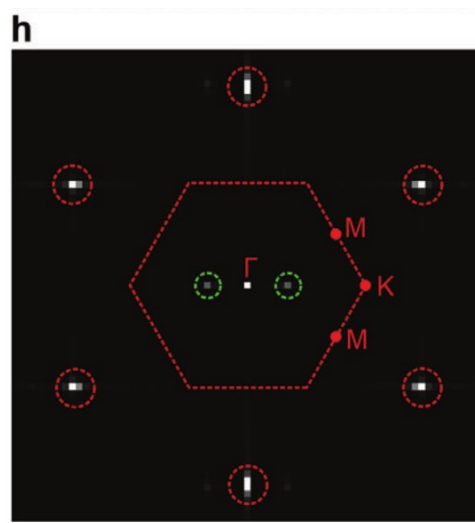


Red peaks →
Atomic lattice

Theory

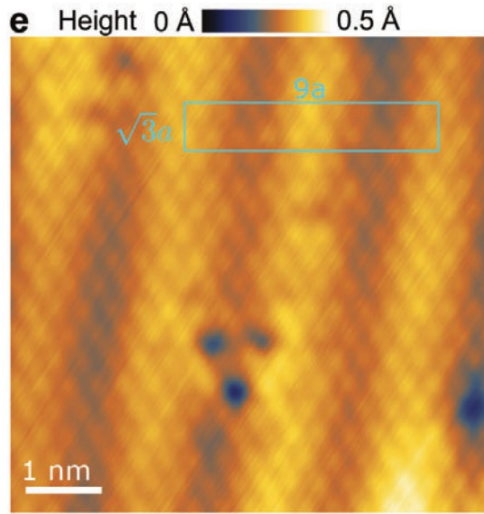


FFT

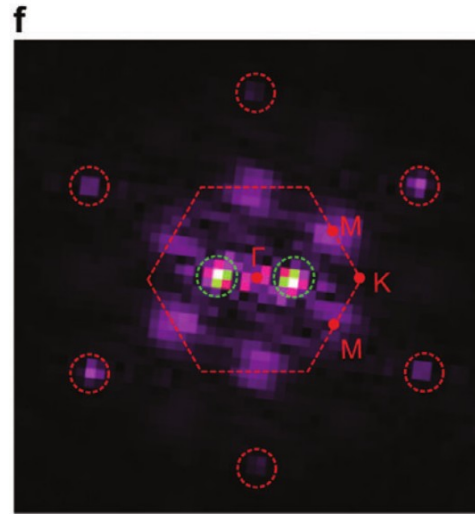


STM characterization of monolayer NiI_2

Experiment



FFT

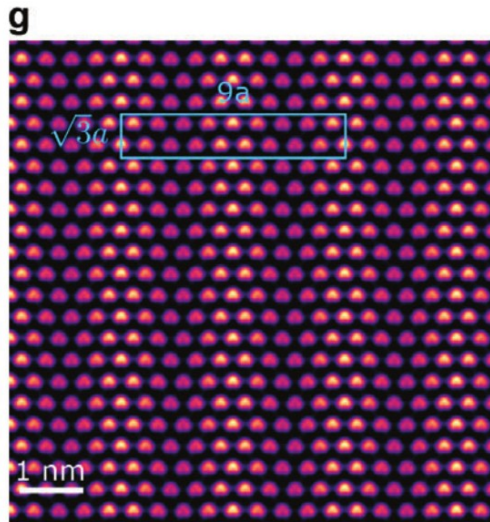


Red peaks \rightarrow
Atomic lattice

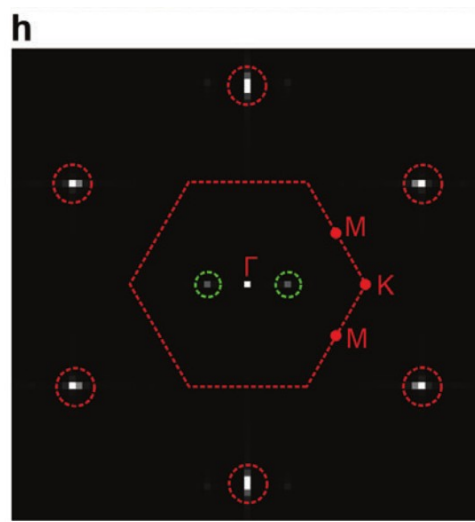
Green peaks \rightarrow
Half of the spin
spiral periodicity

$\mathbf{q} = (0.057, 0.057, 0)$

Theory

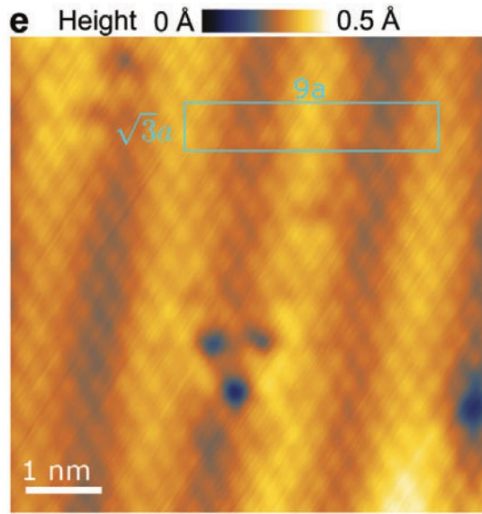


FFT

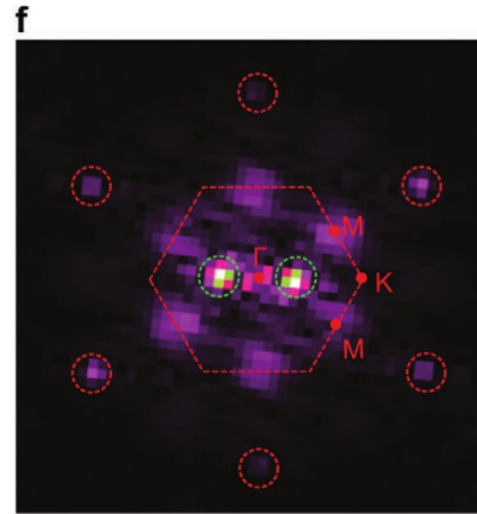


STM characterization of monolayer NiI_2

Experiment



FFT

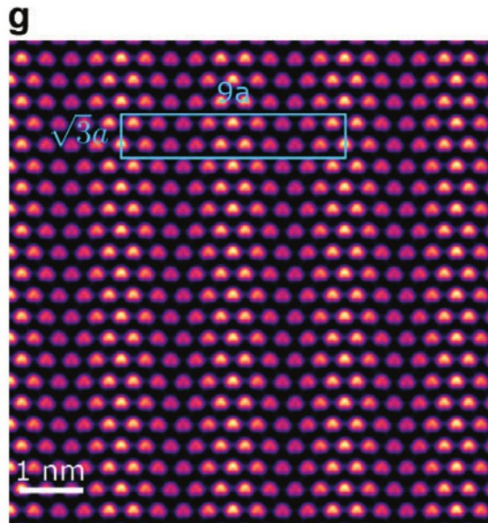


Red peaks \rightarrow
Atomic lattice

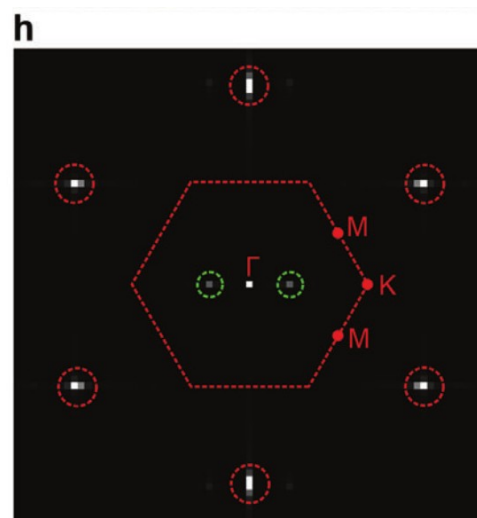
Green peaks \rightarrow
Half of the spin
spiral periodicity

$$\mathbf{q} = (0.057, 0.057, 0)$$

Theory



FFT

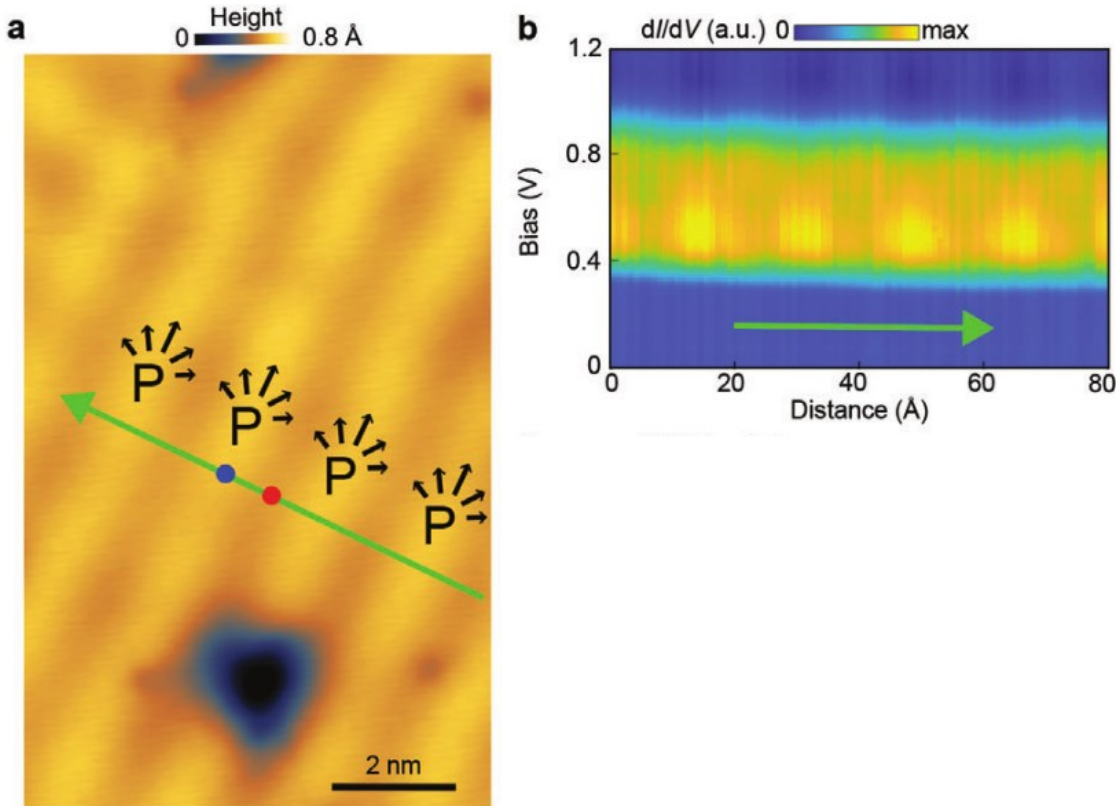


$J_3/J_1 = -0.263$

Characterization
of the spin spiral
magnetic order!

STM characterization of monolayer NiI_2

Inhomogeneous Polarization \rightarrow Band bending of the conduction band

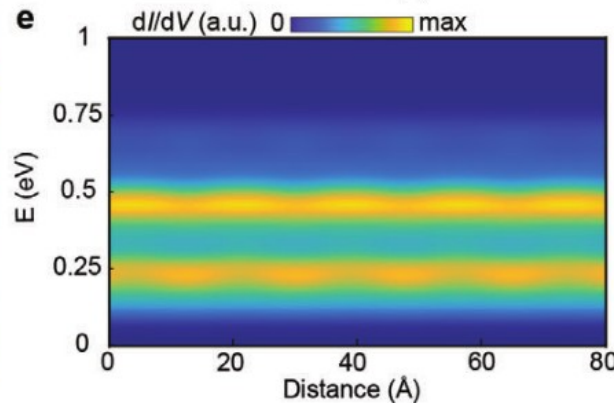
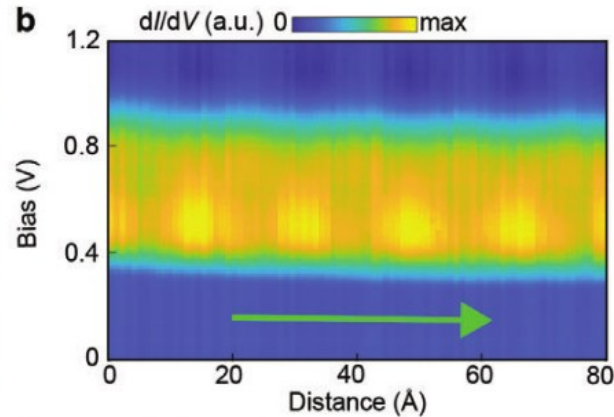
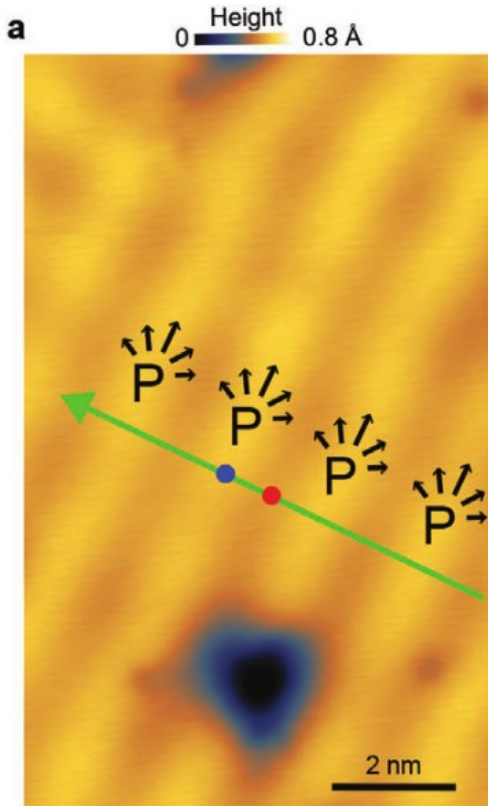


Experiment

Line spectra showing the conduction band

STM characterization of monolayer NiI_2

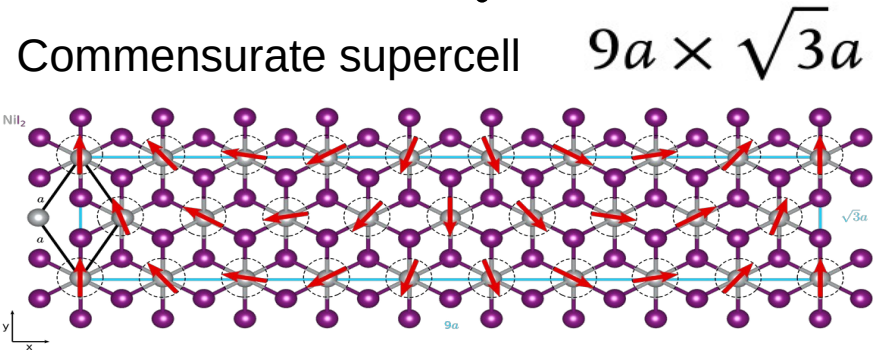
Inhomogeneous Polarization \rightarrow Band bending of the conduction band



Experiment

Line spectra showing the conduction band

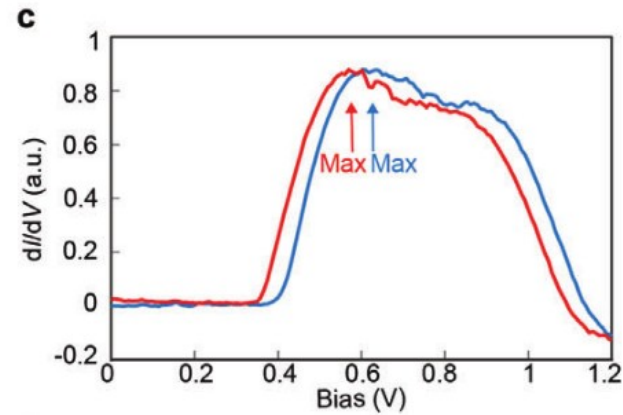
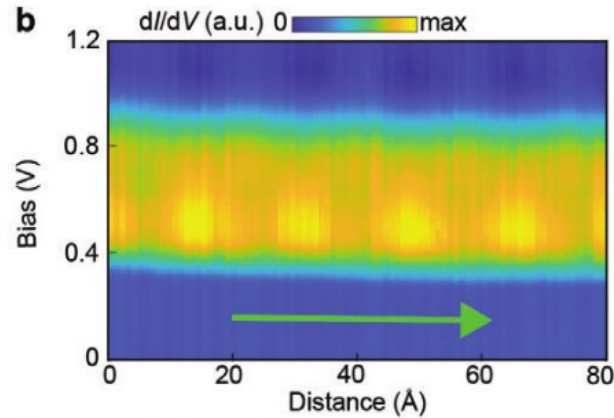
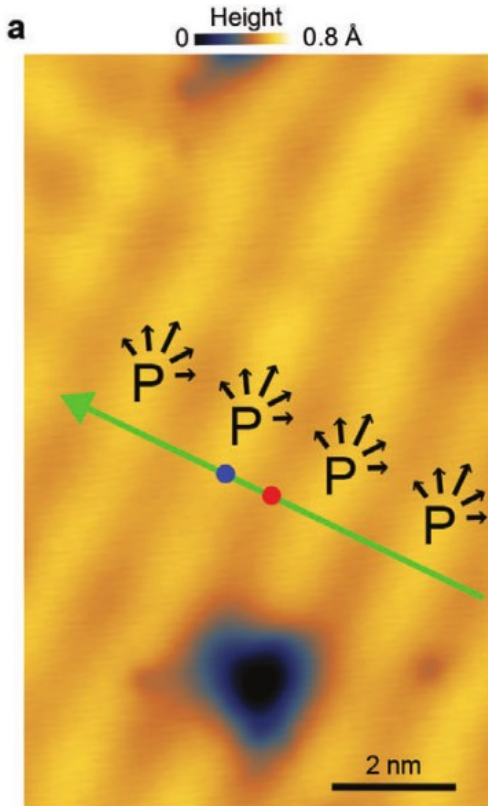
Theory



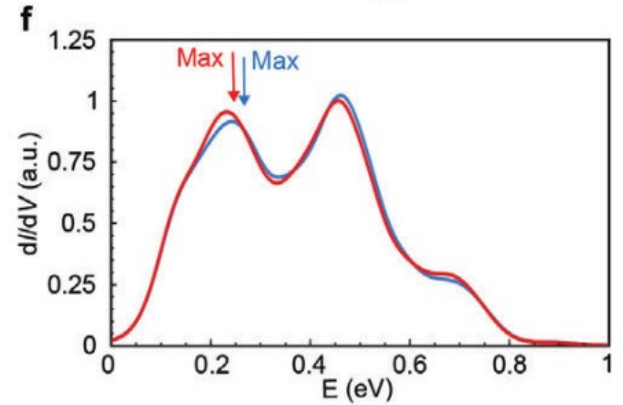
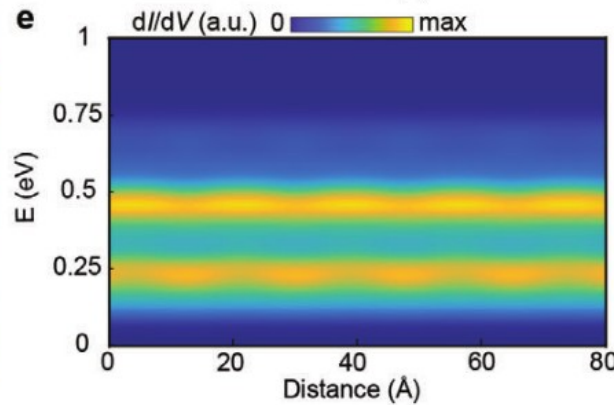
Underestimation of the band gap in DFT,
but the ferroelectric modulation is well captured!

STM characterization of monolayer NiI_2

Inhomogeneous Polarization \rightarrow Band bending of the conduction band



Experiment

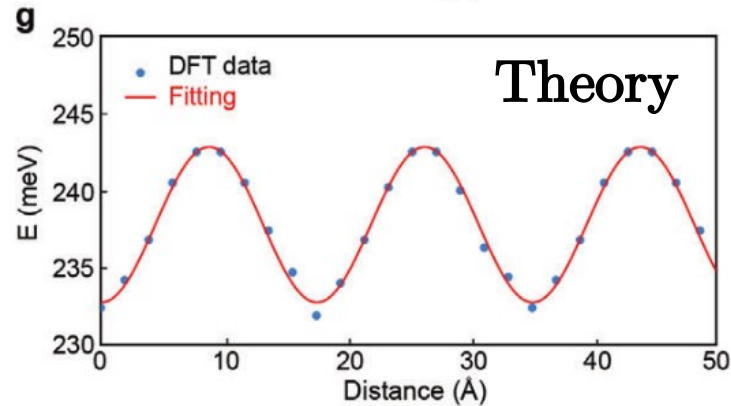
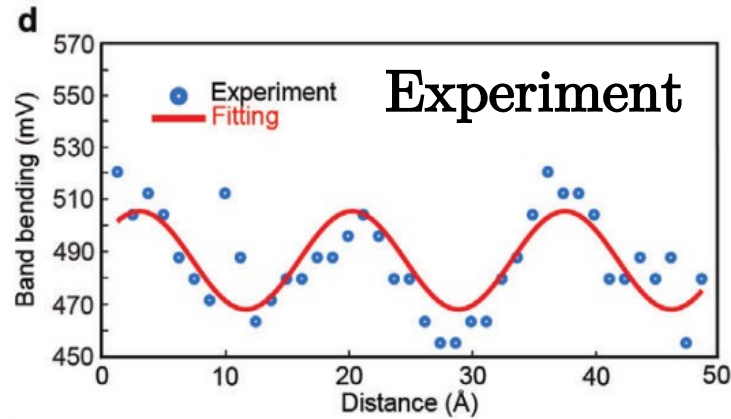
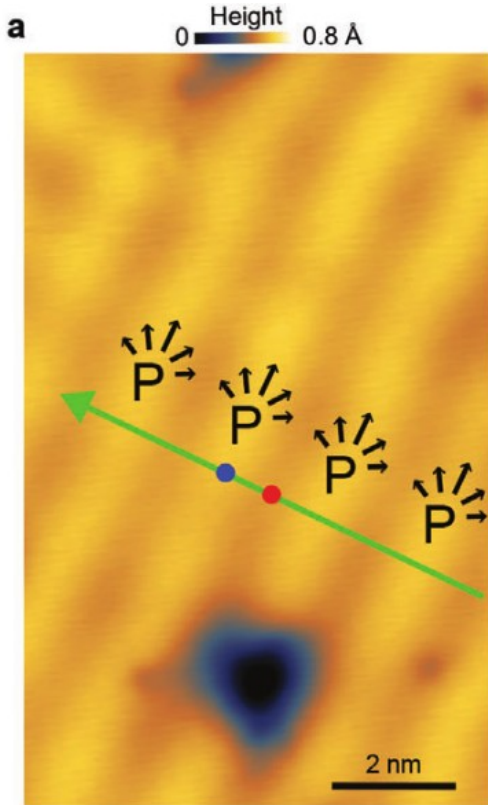


Theory

\rightarrow shift in energy of the conduction band

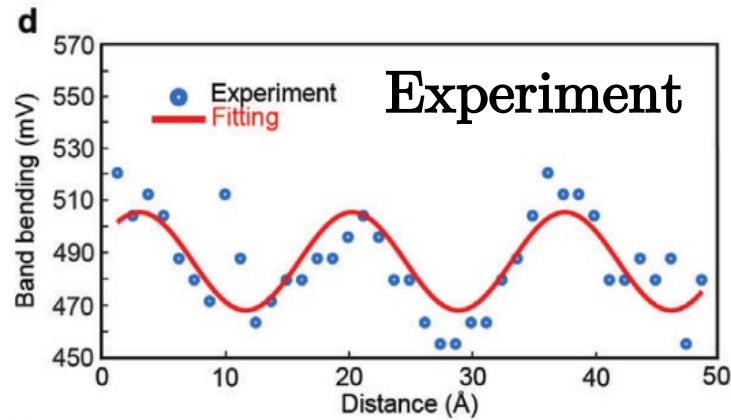
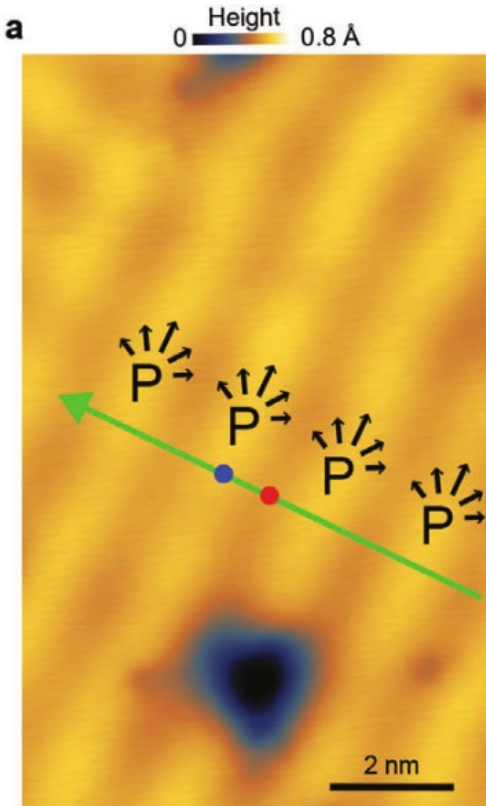
STM characterization of monolayer NiI_2

Inhomogeneous Polarization \rightarrow Band bending of the conduction band



STM characterization of monolayer NiI₂

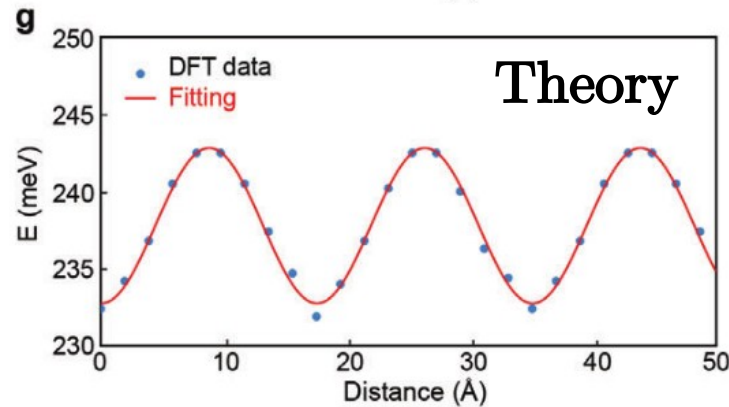
Inhomogeneous Polarization → Band bending of the conduction band



→ Fitting

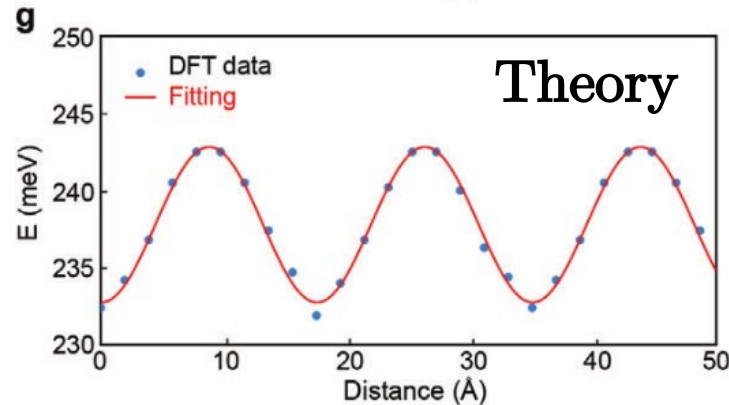
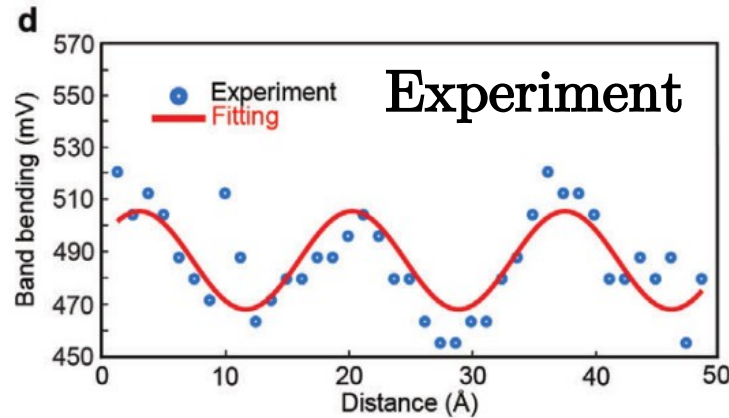
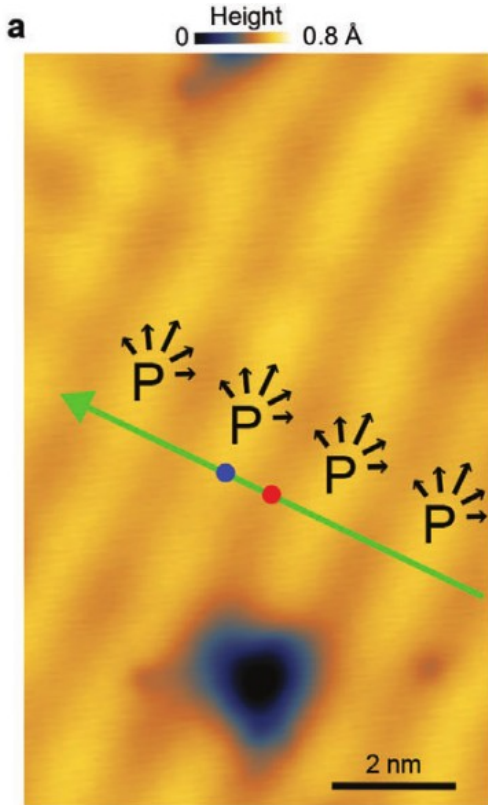
$$E = E_0 + E_P \sin(2\pi x/L_S + \phi)$$

$$E_P = 16.8 \text{ mV}$$



STM characterization of monolayer NiI₂

Inhomogeneous Polarization → Band bending of the conduction band



→ Fitting

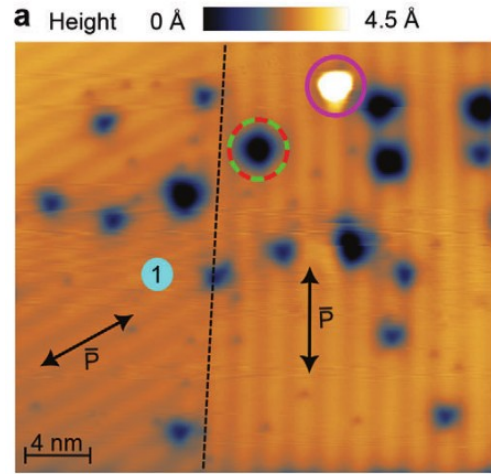
$$E = E_0 + E_P \sin(2\pi x/L_S + \phi)$$

$$E_P = 16.8 \text{ mV}$$

$$P \sim 10^{-12} \text{ C/m}$$

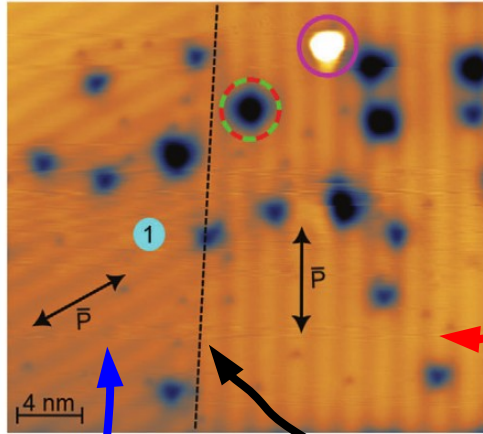
Characterization of the ferroelectric order!

Manipulation of multiferroic domains in monolayer NiI_2



Manipulation of multiferroic domains in monolayer NiI_2

a Height 0 Å 4.5 Å



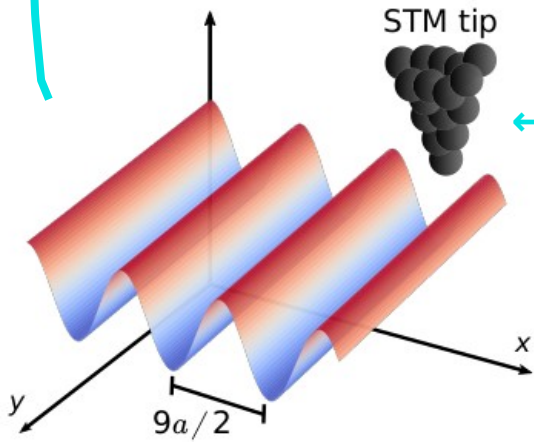
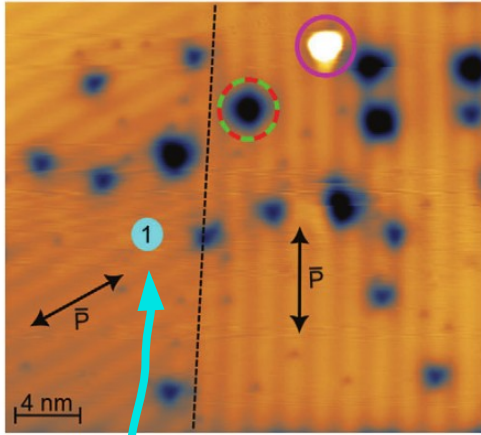
Right
Multiferroic Domain

Multiferroic Domain
Boundary

Left
Multiferroic Domain

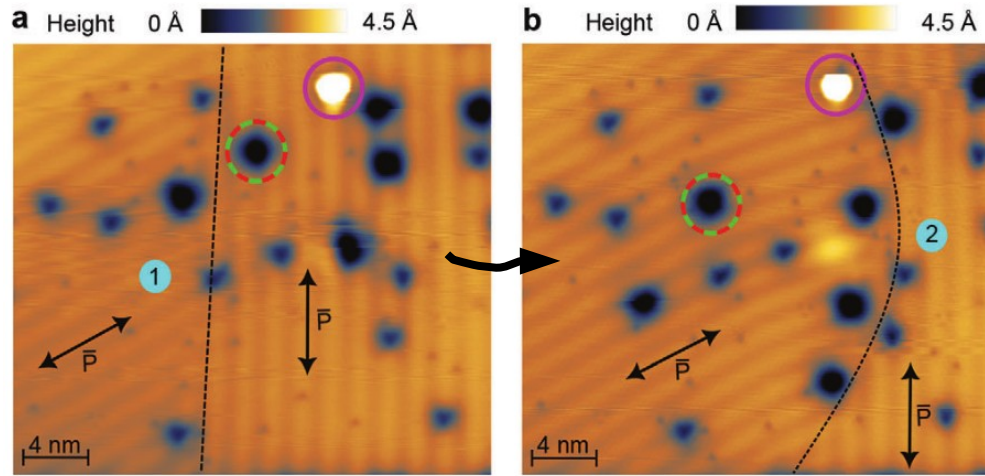
Manipulation of multiferroic domains in monolayer NiI_2

a Height 0 Å 4.5 Å

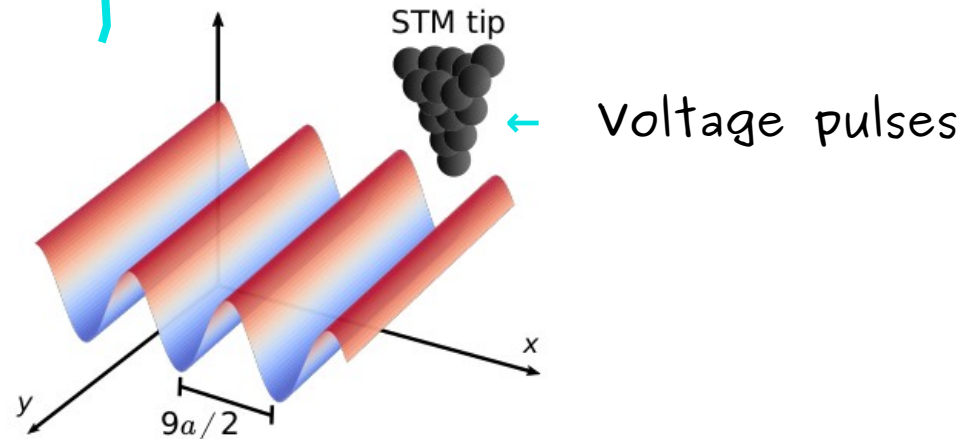
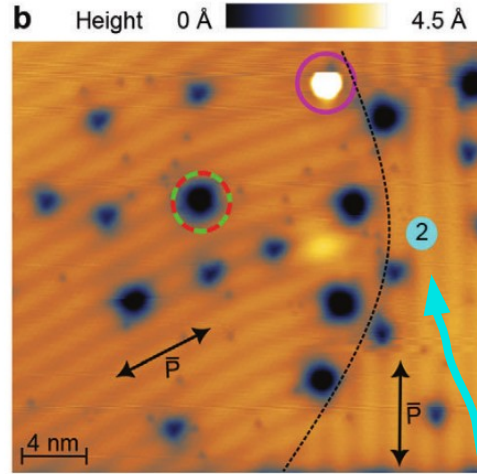
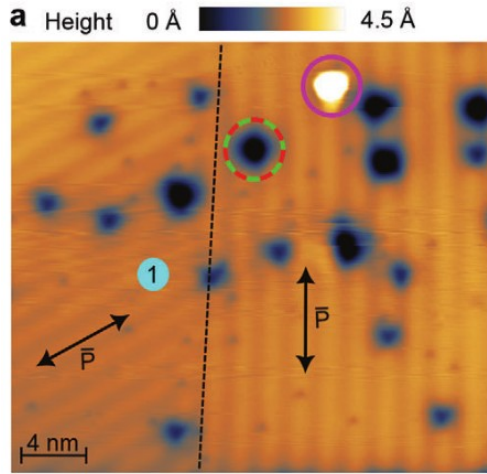


Voltage pulses

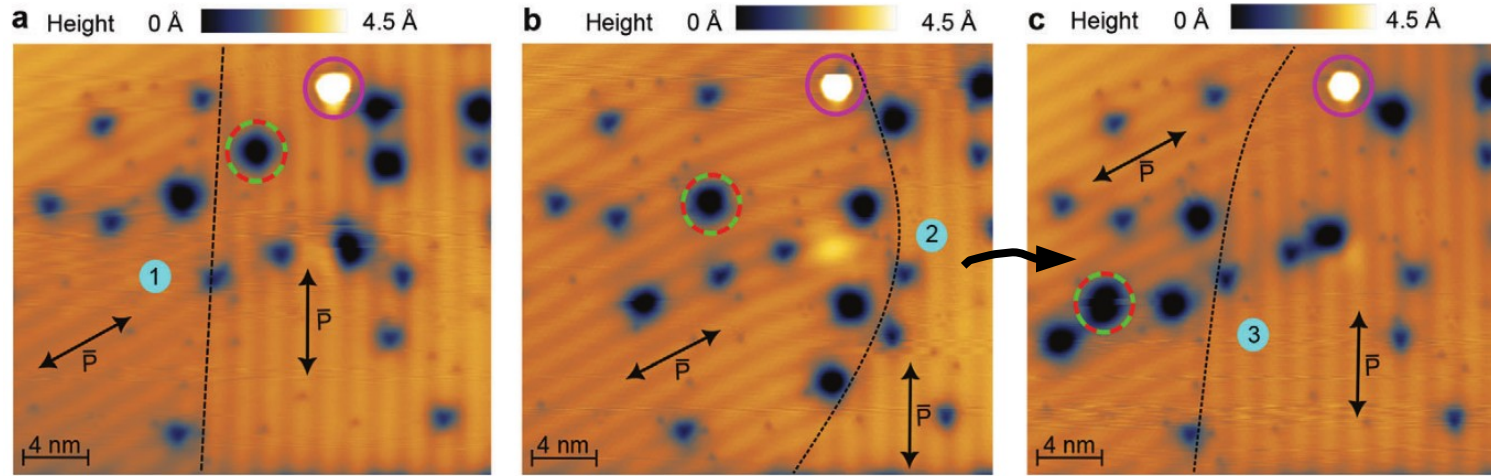
Manipulation of multiferroic domains in monolayer NiI_2



Manipulation of multiferroic domains in monolayer NiI_2

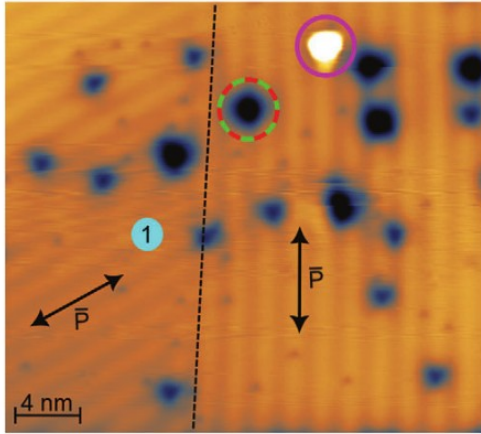


Manipulation of multiferroic domains in monolayer NiI_2

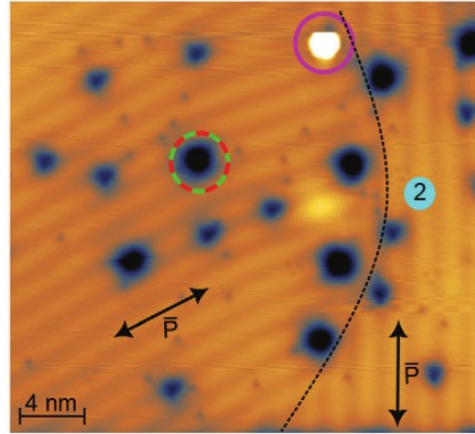


Manipulation of multiferroic domains in monolayer NiI_2

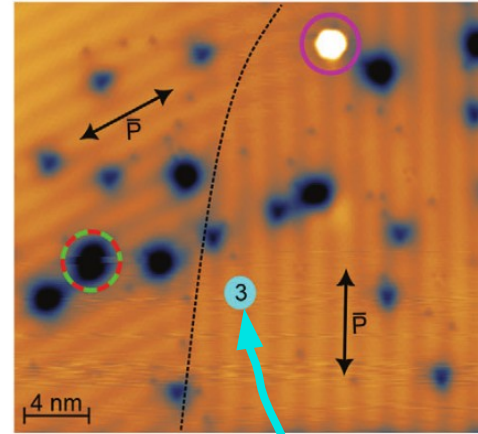
a Height 0 Å 4.5 Å



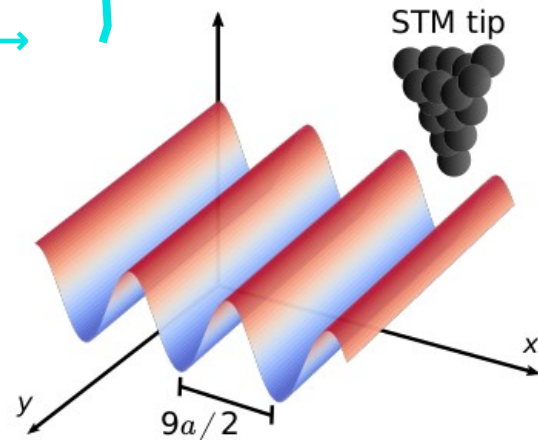
b Height 0 Å 4.5 Å



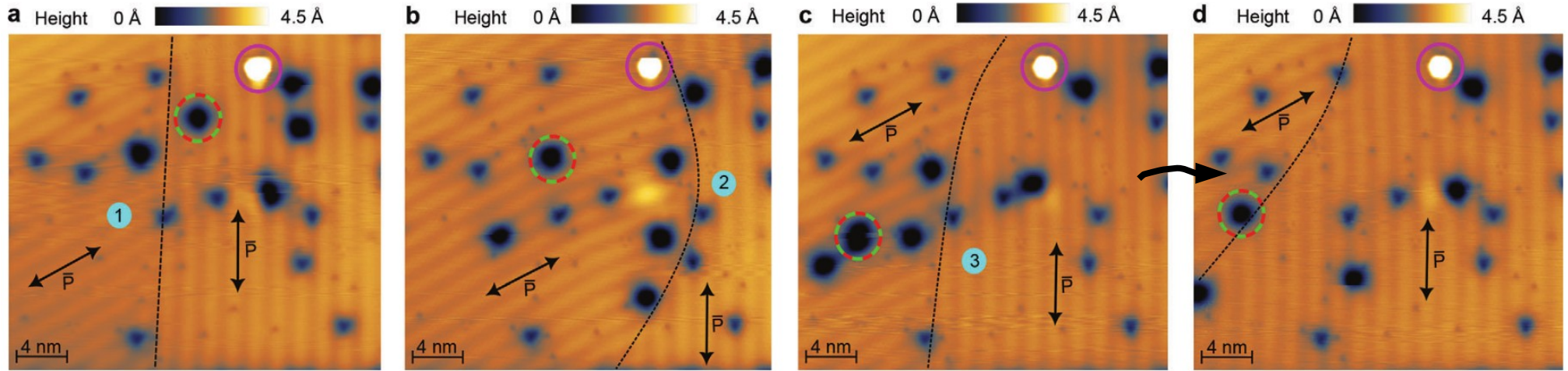
c Height 0 Å 4.5 Å



Voltage pulses →



Manipulation of multiferroic domains in monolayer NiI_2



Manipulation of multiferroic domains!

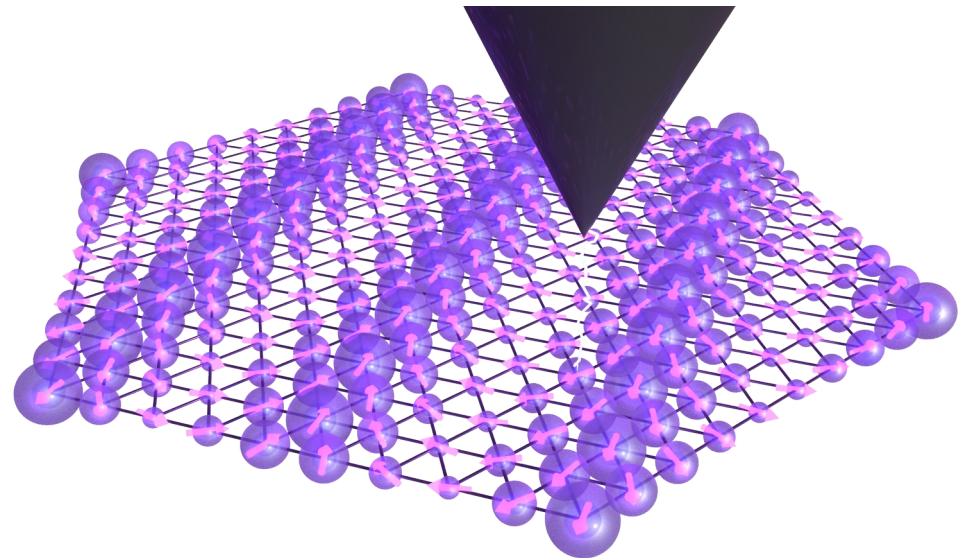
Take home messages

→ The multiferroic order of NiI_2 can stem from the combination of a **spin-spiral order** + a **strong spin-orbit coupling** from I atoms

Adolfo O. Fumega and Jose L. Lado *2D Materials* 9, 025010 (2022)

→ The multiferroic order of NiI_2 can be **demonstrated**, **characterized** and **manipulated** with an STM

Mohammad Amini,* **Adolfo O Fumega**,*
Héctor González-Herrero,
Viliam Vaňo, Shawulienu Kezilebieke,
Jose L Lado⁺, Peter Liljeroth⁺
Advanced Materials 2311342 (2024)



Motivation

Layered van der Waals

Monolayer

Semimetal

Graphene

Insulator

BN

Superconductor

NbSe₂

Ferromagnet

CrI₃

Ferroelectric

MoTe₂

Multiferroic

NiI₂

...

Ingredients
for
Multiferroicity

1) **Non-collinear Magnetism**

+

2) **Spin Orbit Coupling**

Inverse Dzyaloshinskii–Moriya
interaction

$$\mathbf{P}_{ij} = \alpha \lambda_{SOC} (\mathbf{r}_{ij} \times (\mathbf{S}_i \times \mathbf{S}_j))$$

Motivation

Layered van der Waals

Monolayer

Semimetal

Graphene

Insulator

BN

Superconductor

NbSe₂

Ferromagnet

CrI₃

Ferroelectric

MoTe₂

Multiferroic

NiI₂

...

Ingredients
for
Multiferroicity

1) Non-collinear Magnetism

+

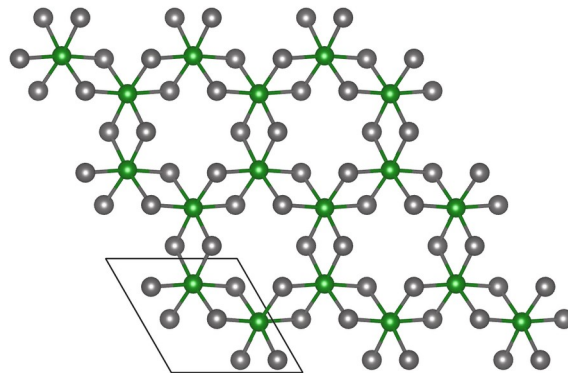
2) Spin Orbit Coupling

Inverse Dzyaloshinskii-Moriya
interaction

$$\mathbf{P}_{ij} = \alpha \lambda_{SOC} (\mathbf{r}_{ij} \times (\mathbf{S}_i \times \mathbf{S}_j))$$

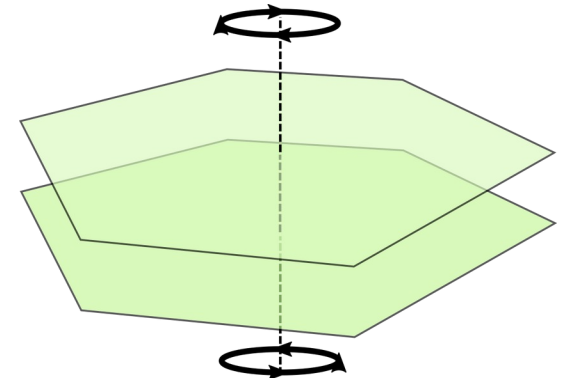
Moiré-driven multiferroic order

CrX₃

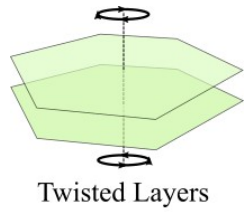


+

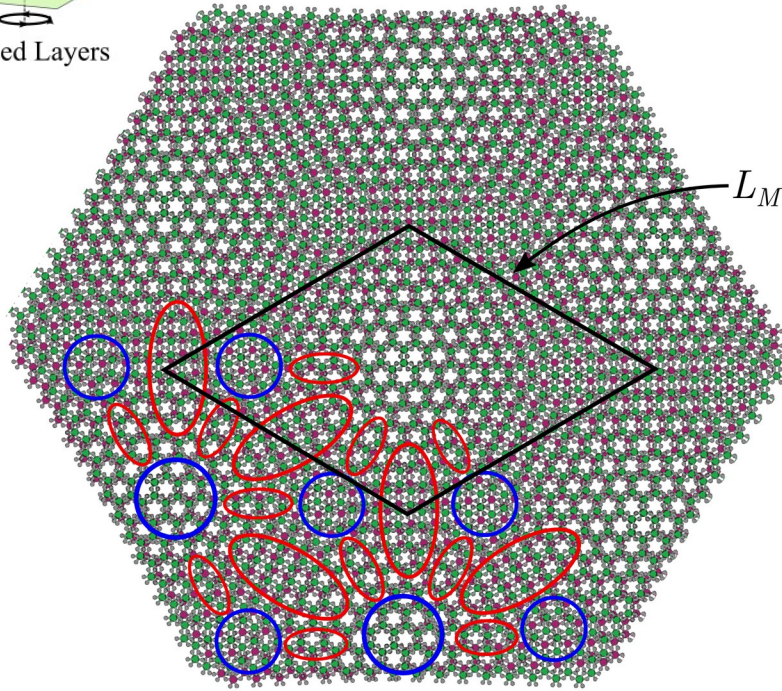
Twisted layers



Twisted CrCl_3 , CrBr_3 and CrI_3 bilayers

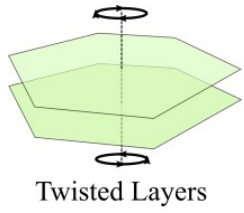


Angle about
 $2^\circ \sim 3^\circ$

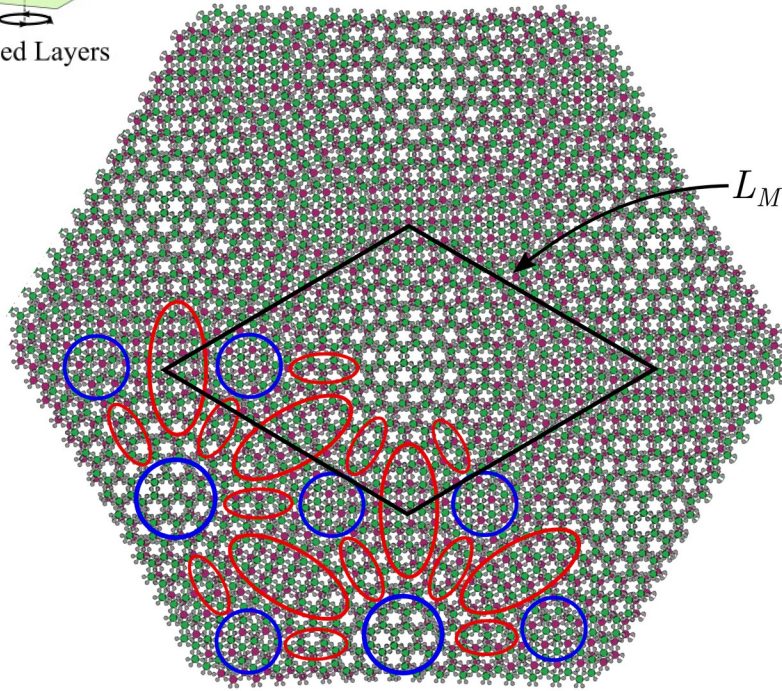


Bilayer Stacking { \textcircled{M} Monoclinic
 \textcircled{R} Rhombohedral

Twisted CrCl_3 , CrBr_3 and CrI_3 bilayers



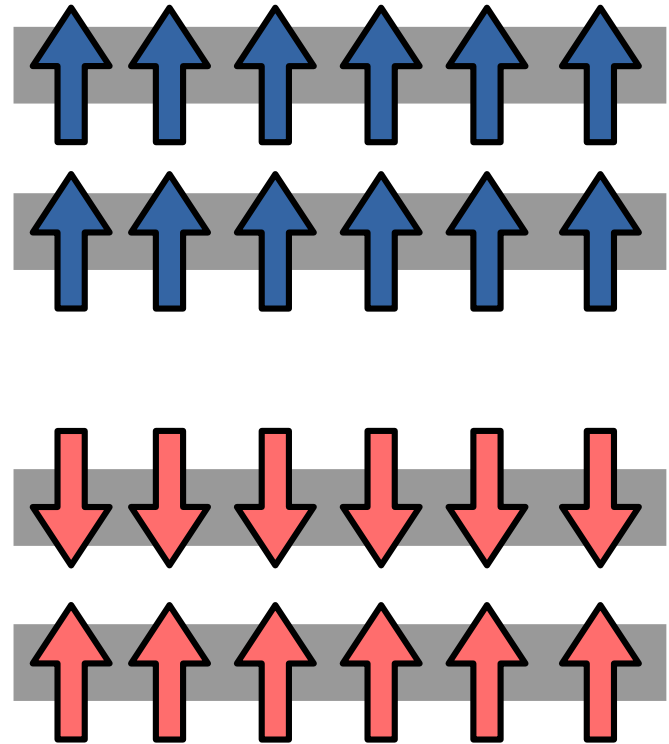
Angle about
 $2^\circ \sim 3^\circ$



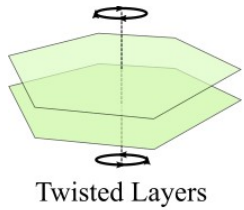
Bilayer Stacking

- (M) Monoclinic
- (R) Rhombohedral

Stacking-dependent Interlayer Magnetic Exchange

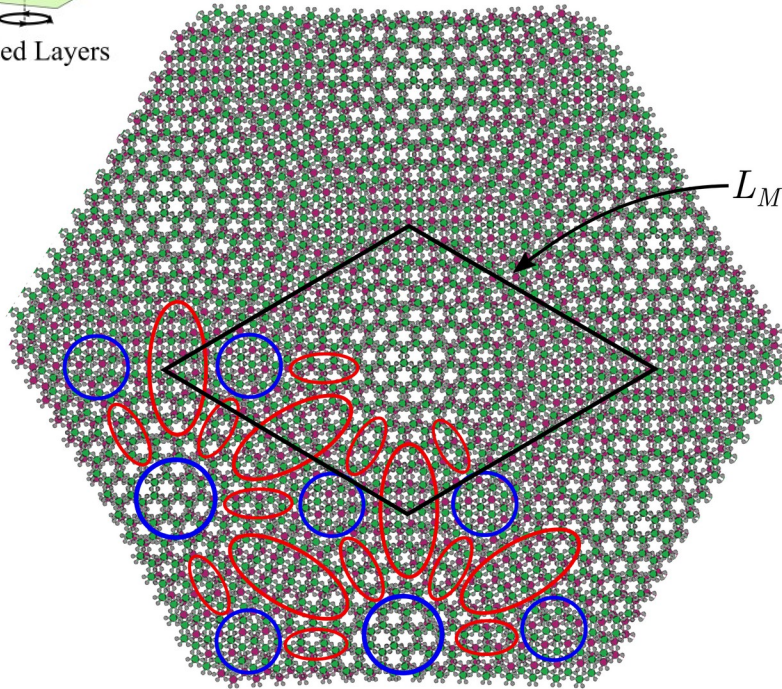


Twisted CrCl_3 , CrBr_3 and CrI_3 bilayers



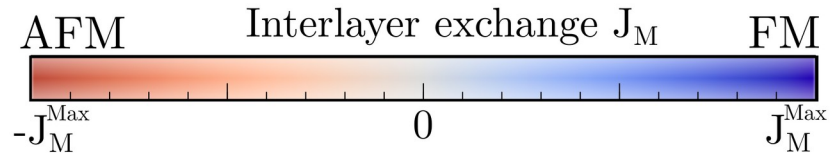
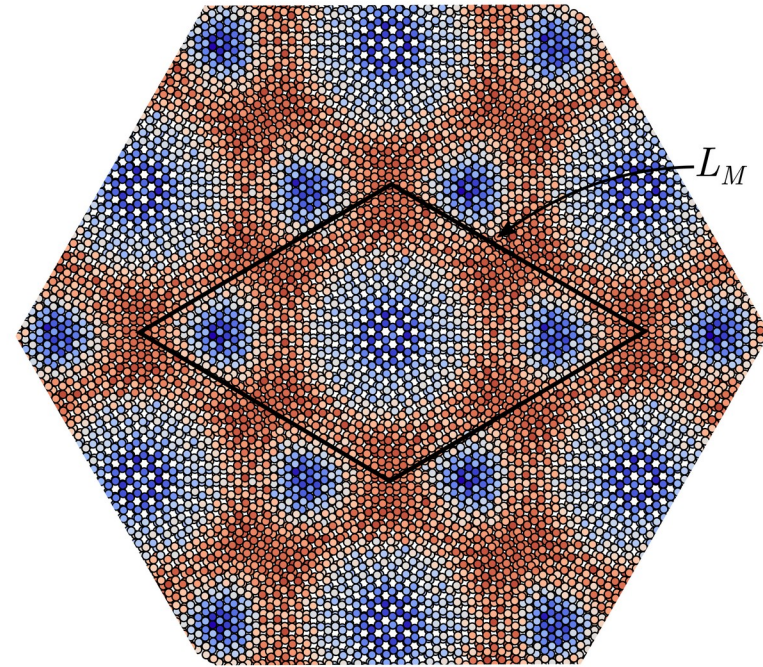
Angle about
 $2^\circ \sim 3^\circ$

Stacking-dependent Interlayer
Magnetic Exchange



Bilayer Stacking

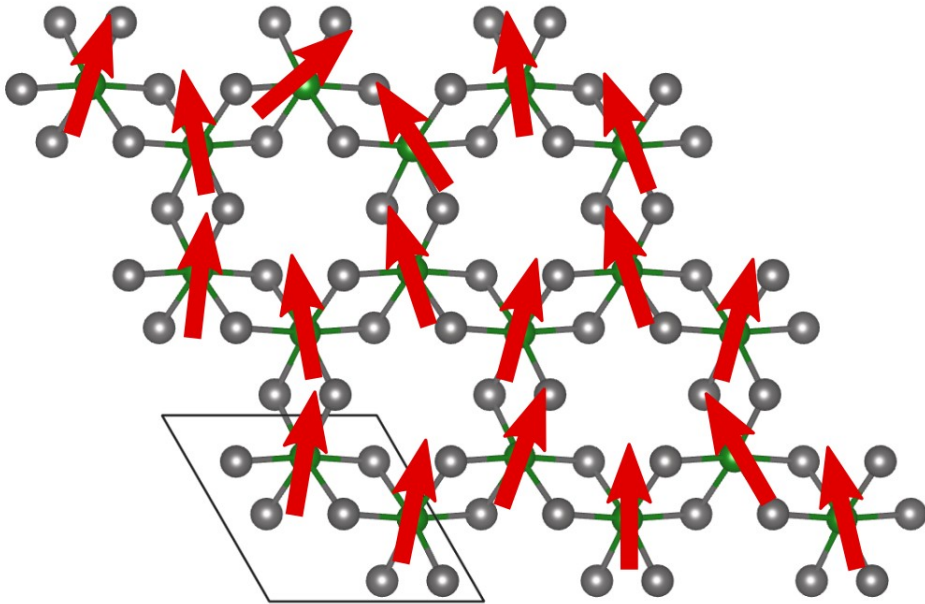
- (M) Monoclinic
- (R) Rhombohedral



Spin Hamiltonian

Intralayer terms

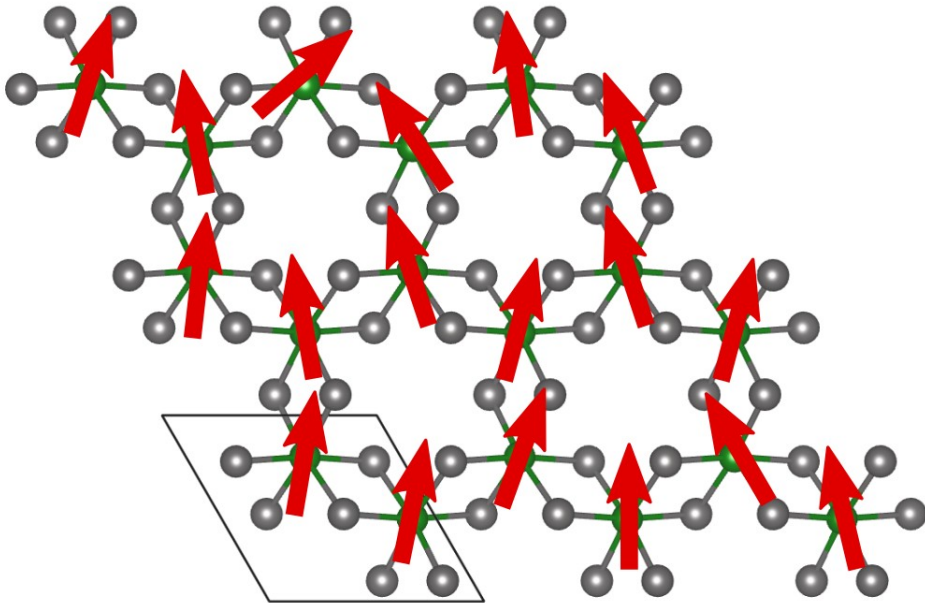
$$\mathcal{H} = -\frac{J}{2} \sum_{\langle i,j \rangle} \mathbf{S}_i \cdot \mathbf{S}_j - \frac{A_v}{2} \sum_{\langle i,j \rangle} S_i^z S_j^z - A_u \sum_i (S_i^z)^2$$



Spin Hamiltonian

Intralayer terms

$$\mathcal{H} = -\frac{J}{2} \sum_{\langle i,j \rangle} \mathbf{S}_i \cdot \mathbf{S}_j - \frac{A_v}{2} \sum_{\langle i,j \rangle} S_i^z S_j^z - A_u \sum_i (S_i^z)^2$$

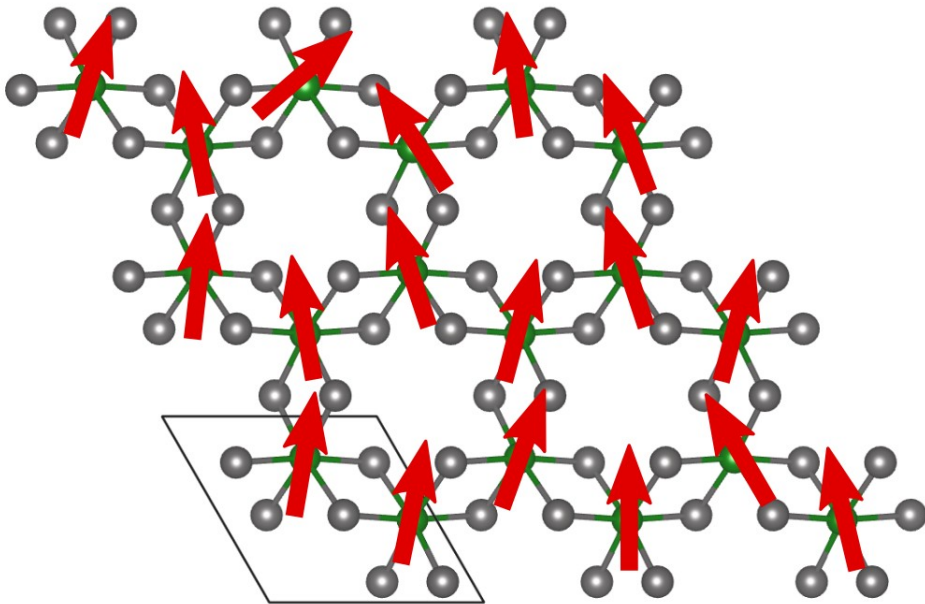


First Neighbor
Ferromagnetic Exchange

Spin Hamiltonian

Intralayer terms

$$\mathcal{H} = -\frac{J}{2} \sum_{\langle i,j \rangle} \mathbf{S}_i \cdot \mathbf{S}_j - \frac{A_v}{2} \sum_{\langle i,j \rangle} S_i^z S_j^z - A_u \sum_i (S_i^z)^2$$

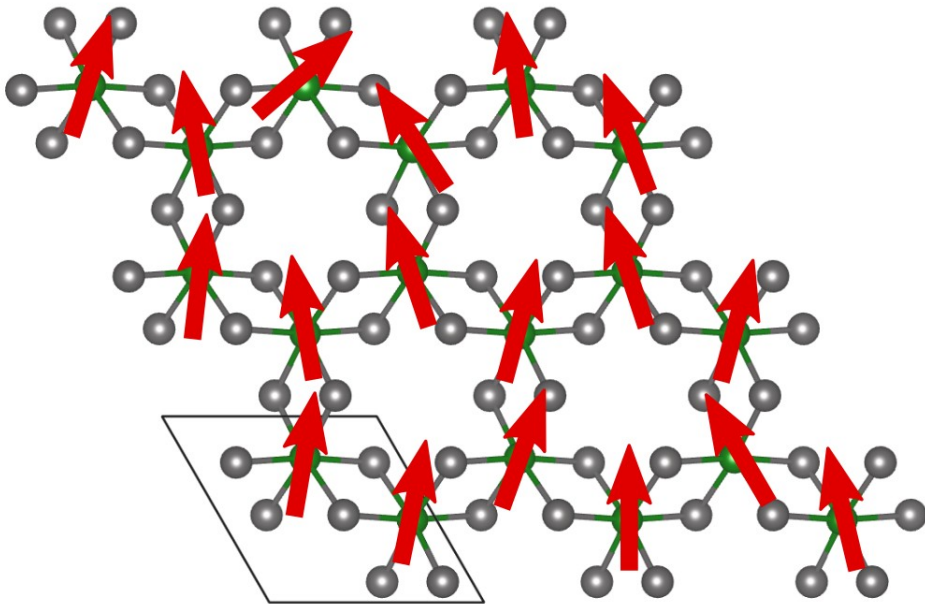


Anisotropic Magnetic
Exchange

Spin Hamiltonian

Intralayer terms

$$\mathcal{H} = -\frac{J}{2} \sum_{\langle i,j \rangle} \mathbf{S}_i \cdot \mathbf{S}_j - \frac{A_v}{2} \sum_{\langle i,j \rangle} S_i^z S_j^z - A_u \sum_i (S_i^z)^2$$

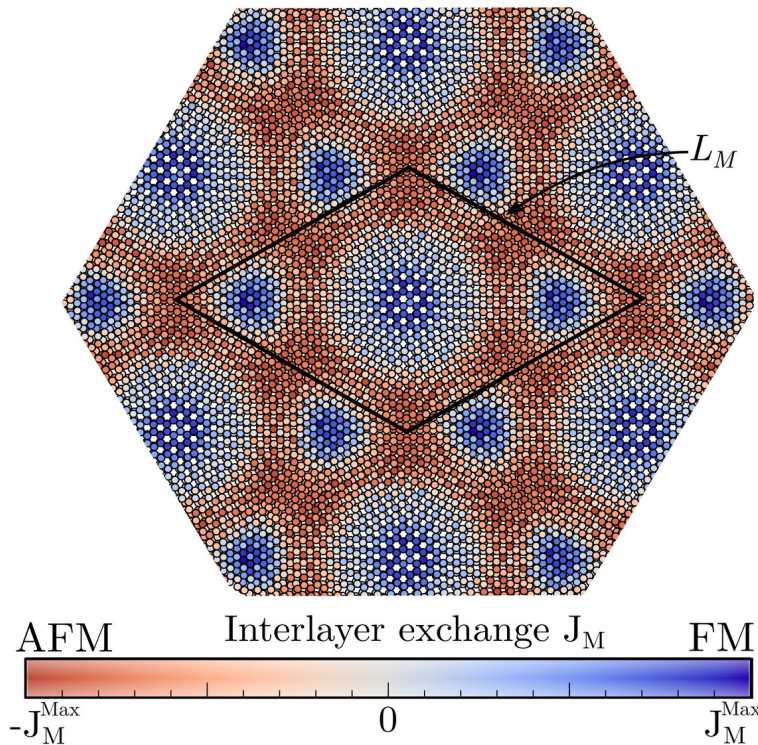


Single Ion Anisotropy

Spin Hamiltonian

Interlayer term

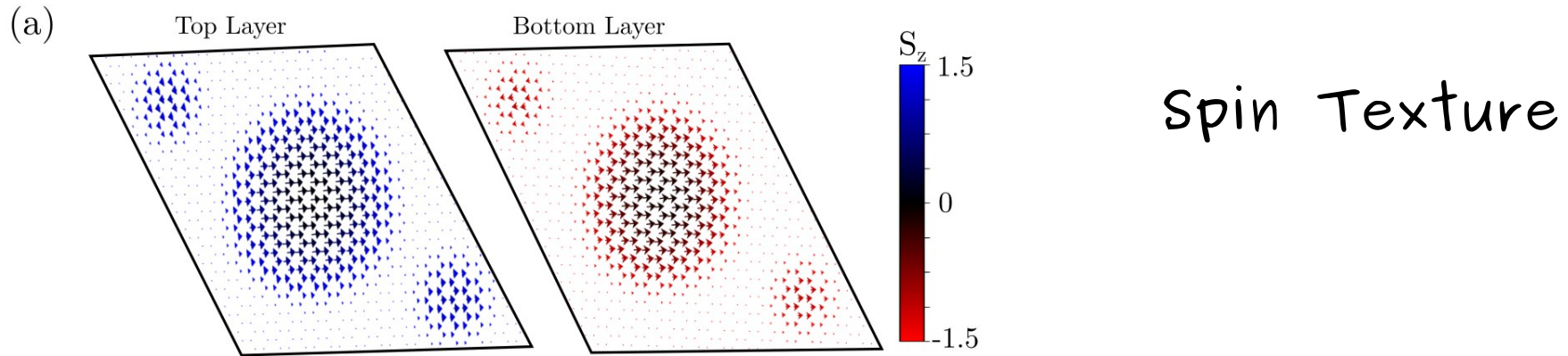
$$\mathcal{H}_{Inter} = -\frac{1}{2} \sum_{i,j} J_M(\mathbf{r}_i, \mathbf{r}_j) \mathbf{S}_i \cdot \mathbf{S}_j$$



Interpolation between
AFM and FM regions using
harmonic functions

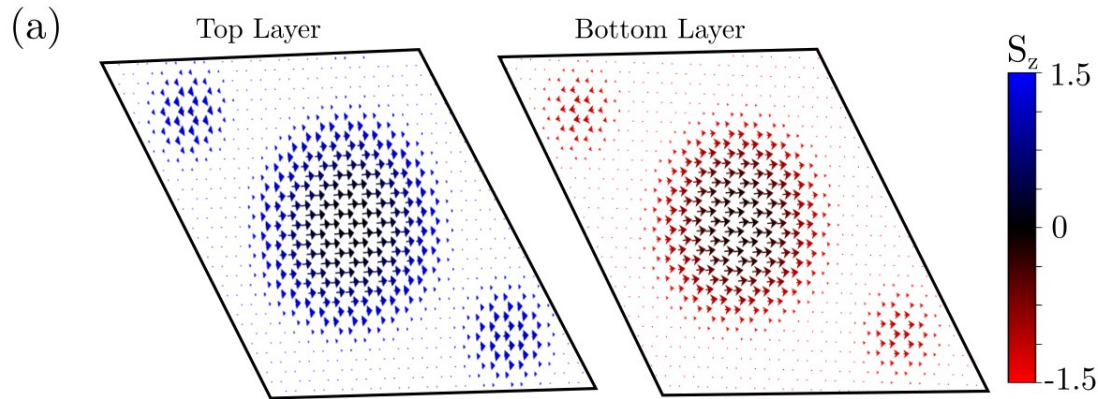
Spin Hamiltonian

Solve the Spin Hamiltonian \rightarrow Ground State



Spin Hamiltonian

Solve the Spin Hamiltonian \rightarrow Ground State



Spin Texture



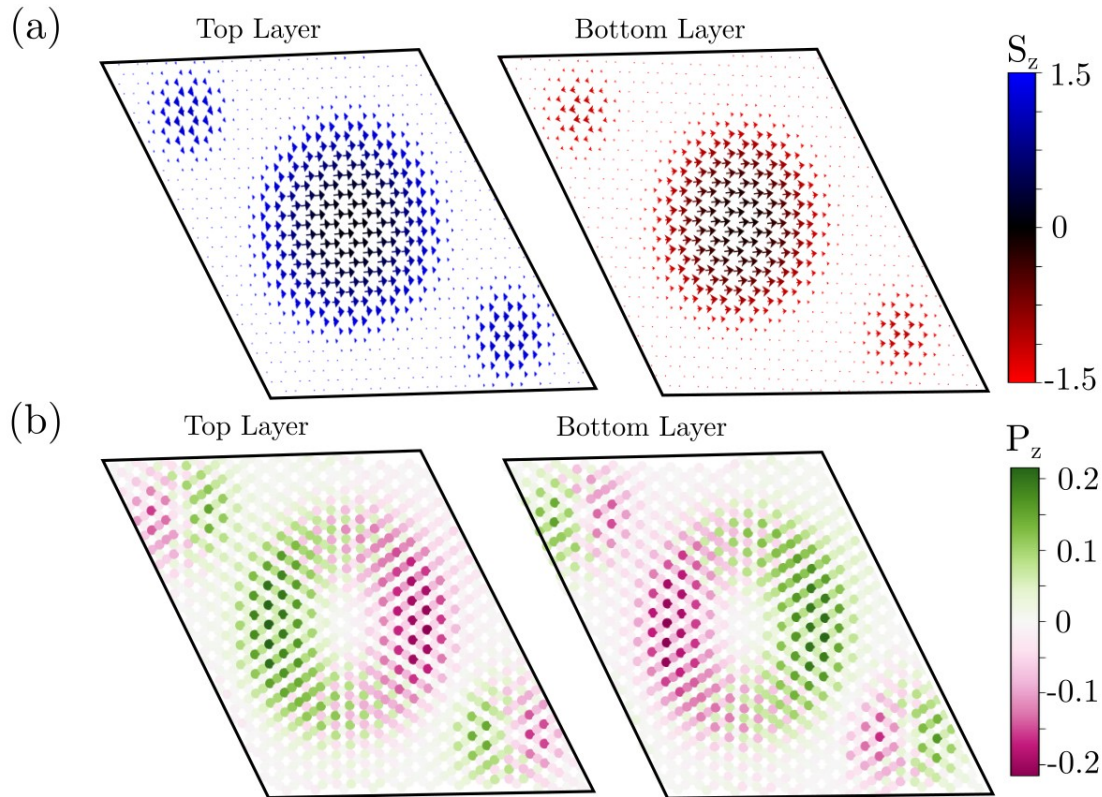
Electric Polarization

$$\mathbf{P}_{ij} = \alpha \lambda_{SOC} (\mathbf{r}_{ij} \times (\mathbf{S}_i \times \mathbf{S}_j))$$

Inverse Dzyaloshinskii–Moriya interaction

Spin Hamiltonian

Solve the Spin Hamiltonian \rightarrow Ground State



Spin Texture



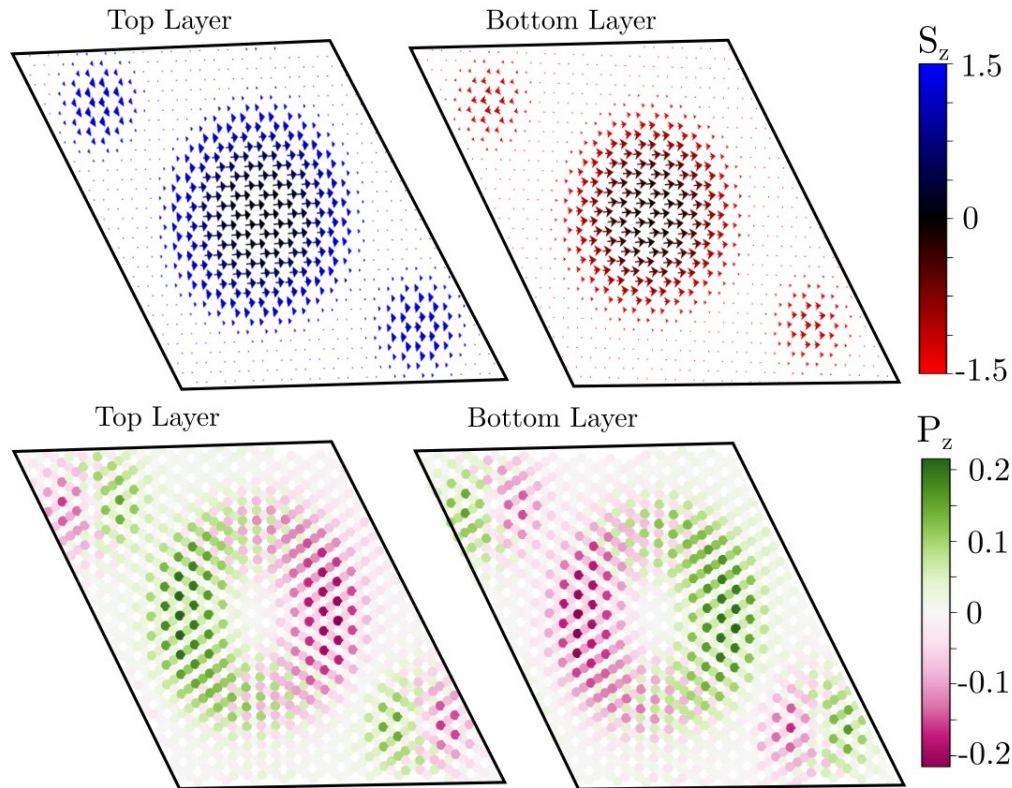
Electric Polarization

$$\mathbf{P}_{ij} = \alpha \lambda_{SOC} (\mathbf{r}_{ij} \times (\mathbf{S}_i \times \mathbf{S}_j))$$

Inverse Dzyaloshinskii-Moriya interaction

Spin Hamiltonian

Considering the different parameters: λ_{soc} and A_v



Which CrX_3 displays
the strongest
multiferroic order?

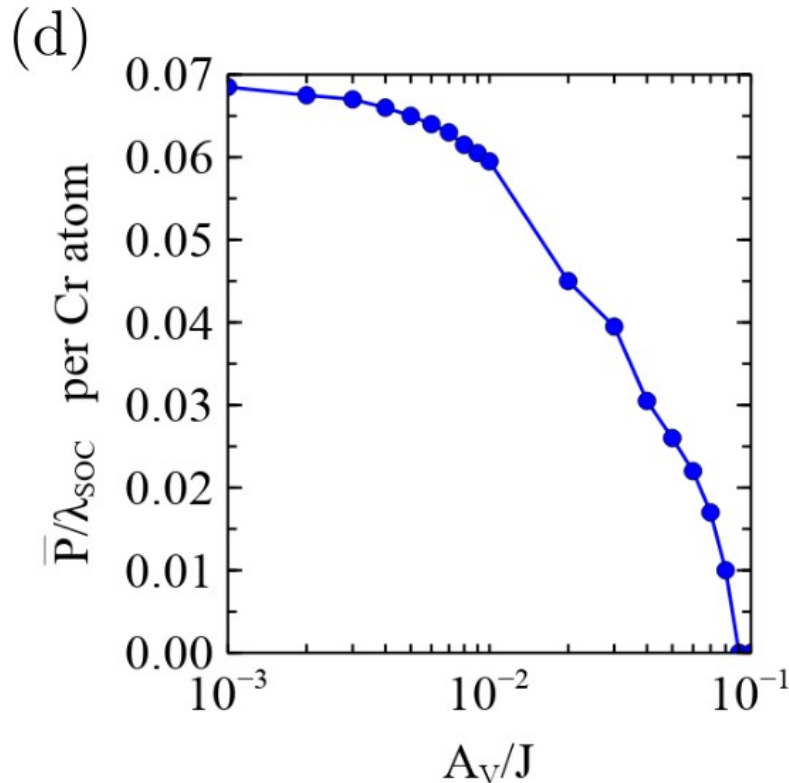
Spin Hamiltonian

Parameters dependence

Anisotropic Exchange

Electric Polarization

$$\mathbf{P}_{ij} = \alpha \lambda_{SOC} (\mathbf{r}_{ij} \times (\mathbf{S}_i \times \mathbf{S}_j))$$



$A_v \rightarrow$ Collinearity \rightarrow Decrease P

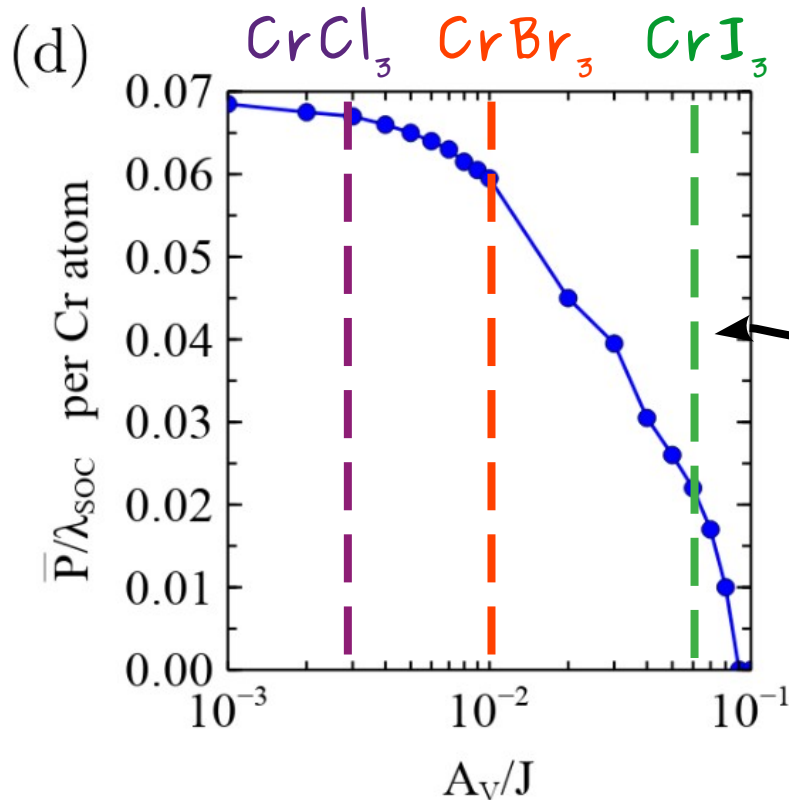
Spin Hamiltonian

Parameters dependence

Anisotropic Exchange

Electric Polarization

$$\mathbf{P}_{ij} = \alpha \lambda_{SOC} (\mathbf{r}_{ij} \times (\mathbf{S}_i \times \mathbf{S}_j))$$

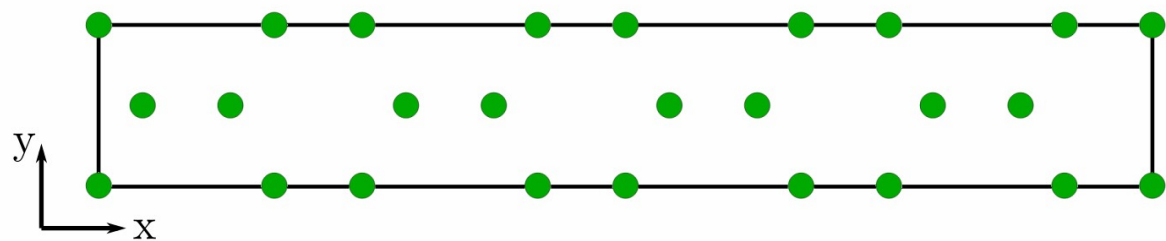


$A_v \rightarrow$ Collinearity \rightarrow Decrease P

CrI_3 in the verge of displaying a multiferroic behavior due to the strong anisotropy

Ab initio calculations

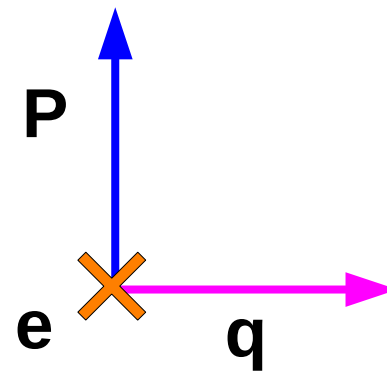
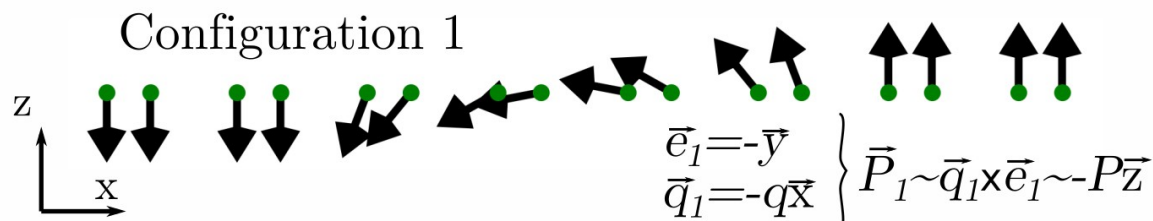
Electric polarization in a spin texture of CrX_3



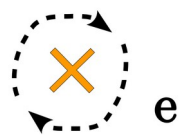
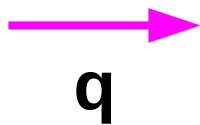
$$\mathbf{P}_{ij} = \alpha \lambda_{SOC} (\mathbf{r}_{ij} \times (\mathbf{S}_i \times \mathbf{S}_j))$$

Electric Polarization

$$\mathbf{P} = \beta \lambda_{SOC} (\mathbf{q} \times \mathbf{e})$$

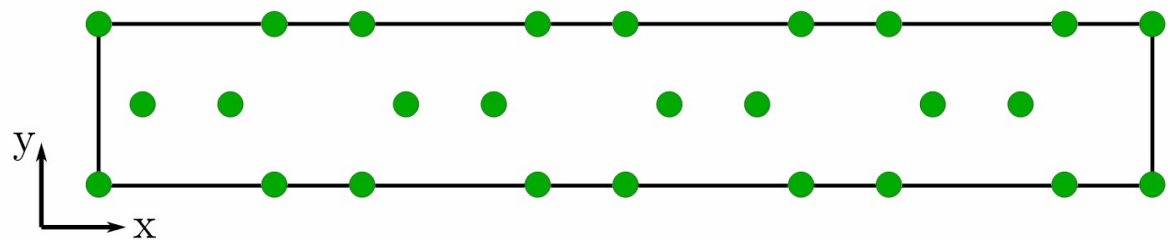


Propagation vector Rotation vector

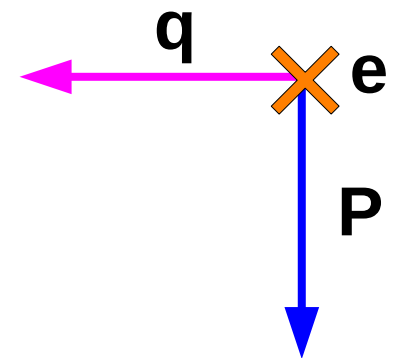
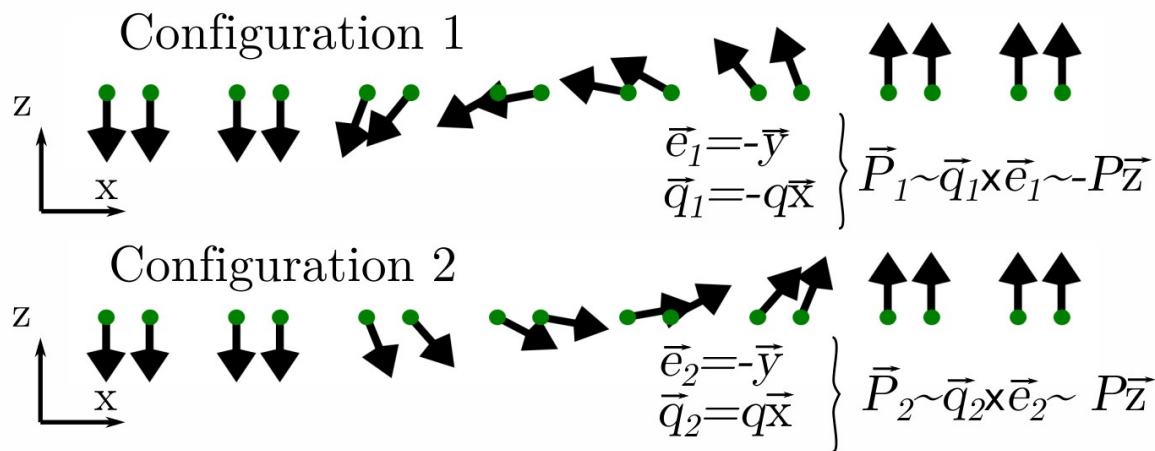


Ab initio calculations

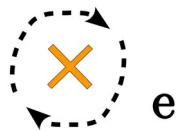
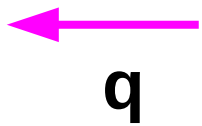
Electric polarization in a spin texture of CrX_3



Electric Polarization
 $\mathbf{P} = \beta \lambda_{SOC} (\mathbf{q} \times \mathbf{e})$

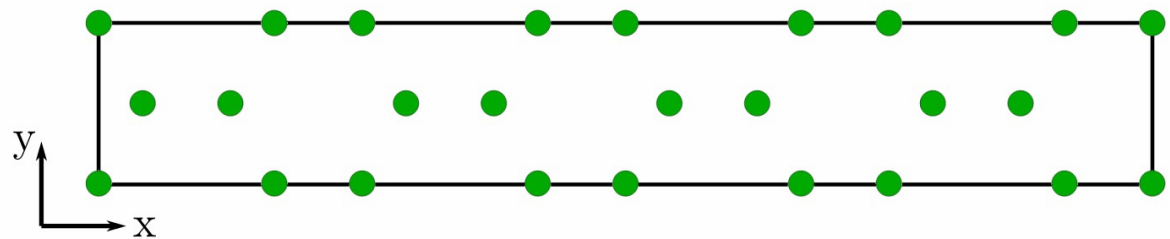


Propagation vector Rotation vector



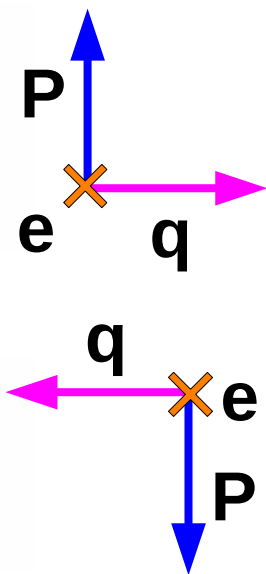
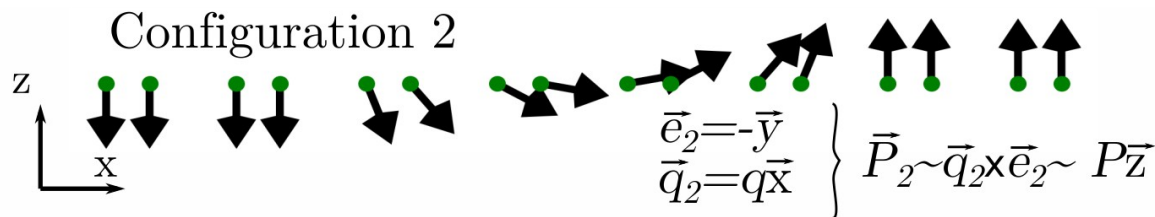
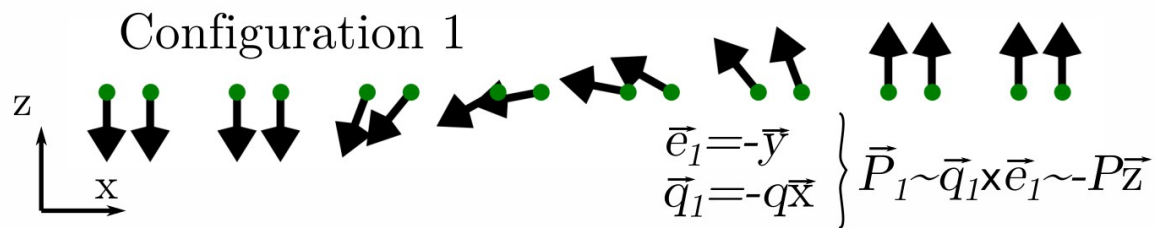
Ab initio calculations

Electric polarization in a spin texture of CrX_3



Electric Polarization

$$\mathbf{P} = \beta \lambda_{SOC} (\mathbf{q} \times \mathbf{e})$$



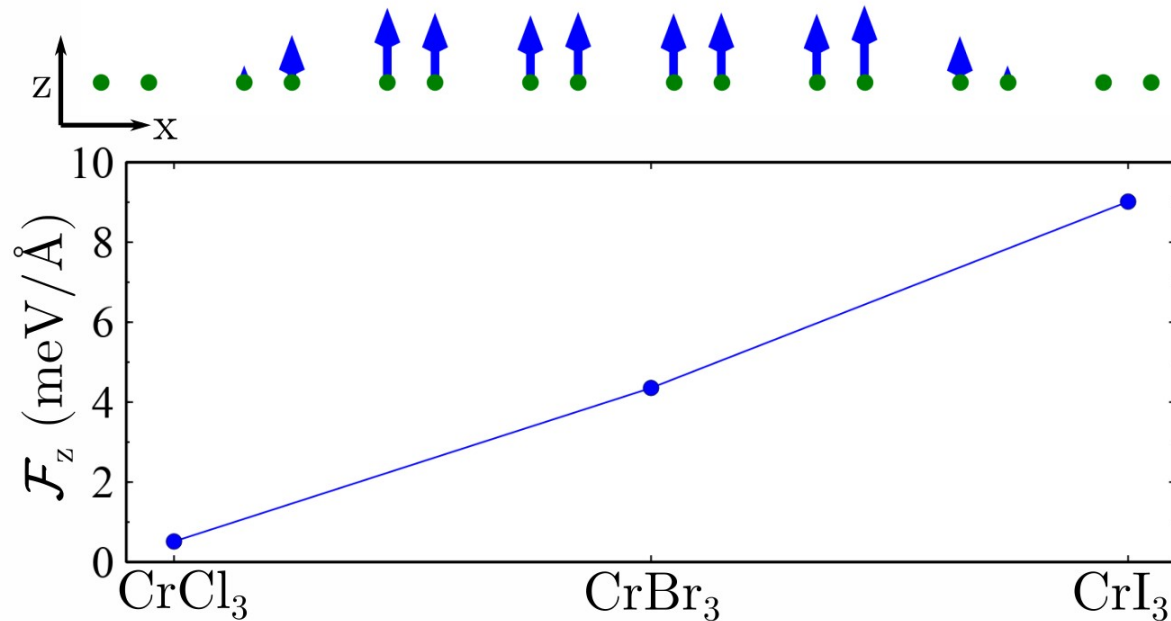
Difference between configurations

Signature of Ferroelectricity

Ab initio calculations

Electric polarization in a spin texture of CrX_3

Ferroelectric force difference



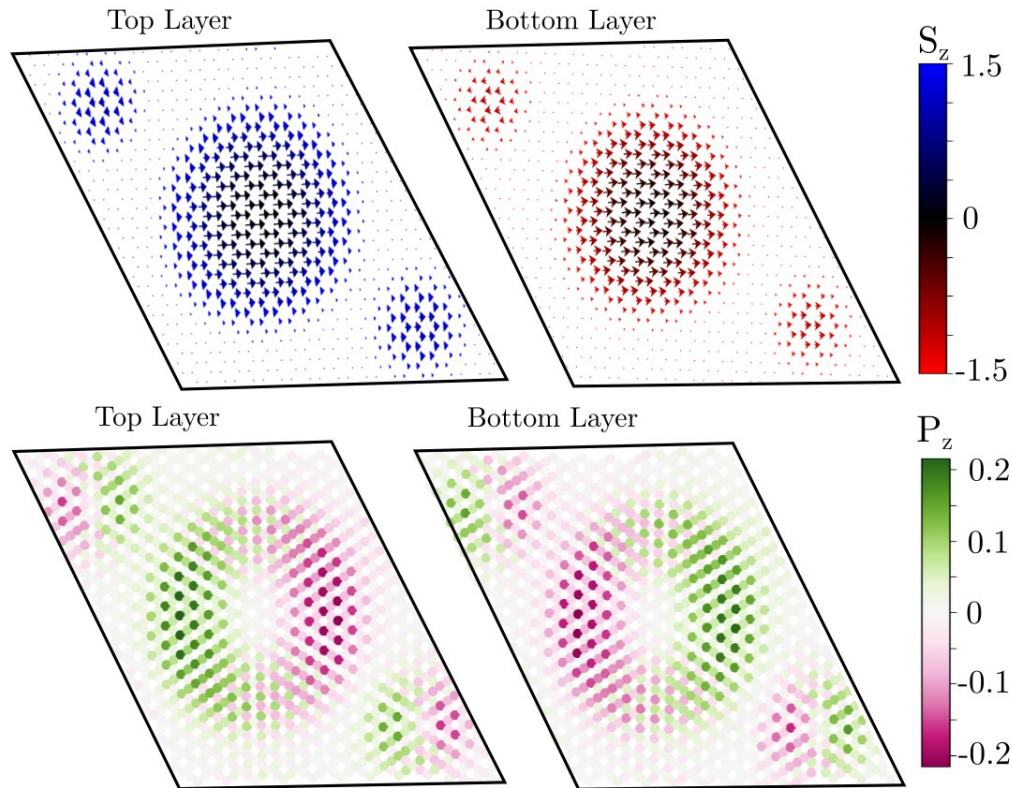
Going down in the
halide group

↓
Increase SOC

↓
Increase
Ferroelectric force

Spin Hamiltonian

Considering the different parameters: λ_{soc} and A_v



CrBr_3 displays
the strongest
multiferroic order

Spin Hamiltonian

Magnetolectric Coupling

$$\mathcal{H}_E = \frac{1}{2} \sum_{ij} \mathbf{E} \cdot \mathbf{P}_{ij}$$

External Electric field

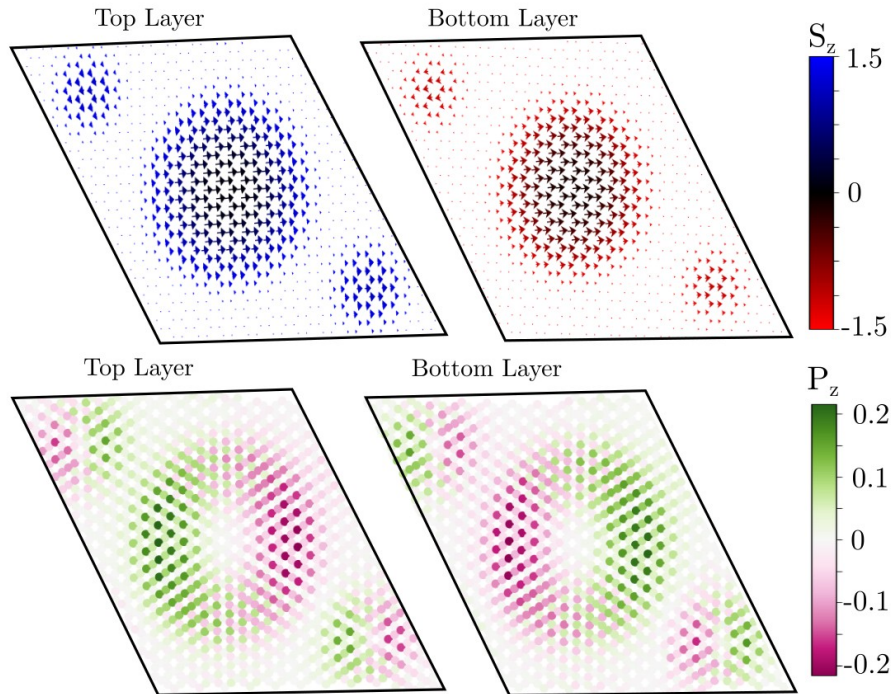
Spin Hamiltonian

Magnetoelectric Coupling

External Electric field

$$\mathcal{H}_E = \frac{1}{2} \sum_{ij} \mathbf{E} \cdot \mathbf{P}_{ij}$$

$E/J=0$



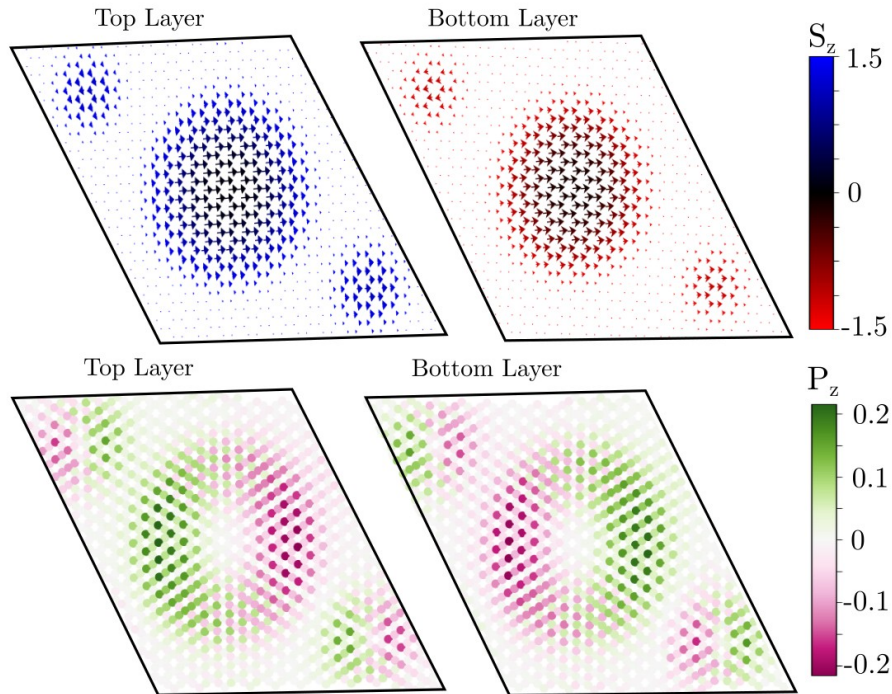
Spin Hamiltonian

Magnetolectric Coupling

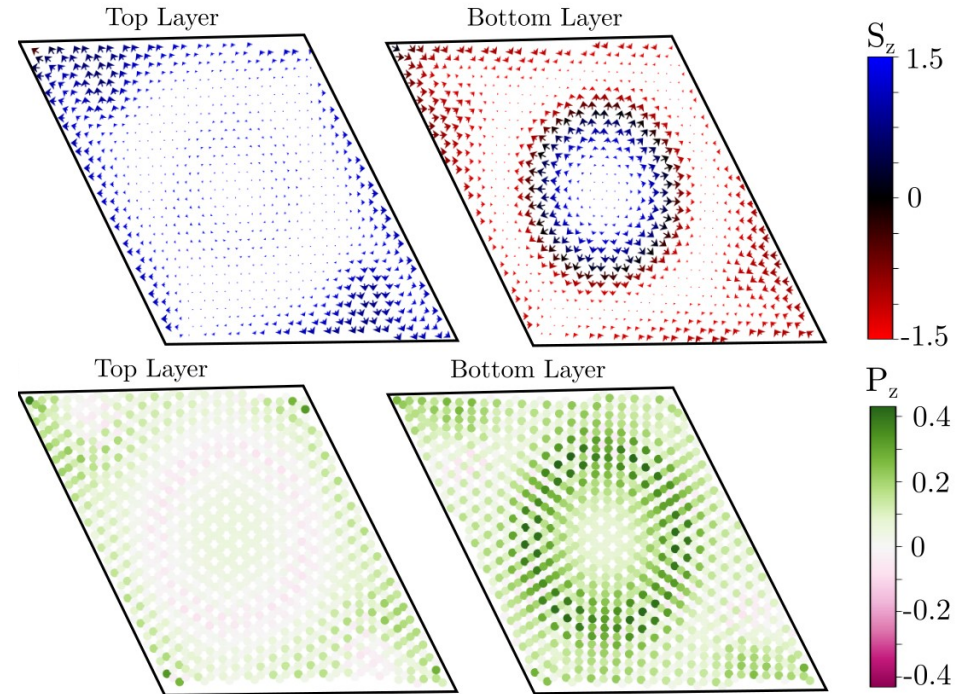
$$\mathcal{H}_E = \frac{1}{2} \sum_{ij} \mathbf{E} \cdot \mathbf{P}_{ij}$$

External Electric field

$E/J=0$



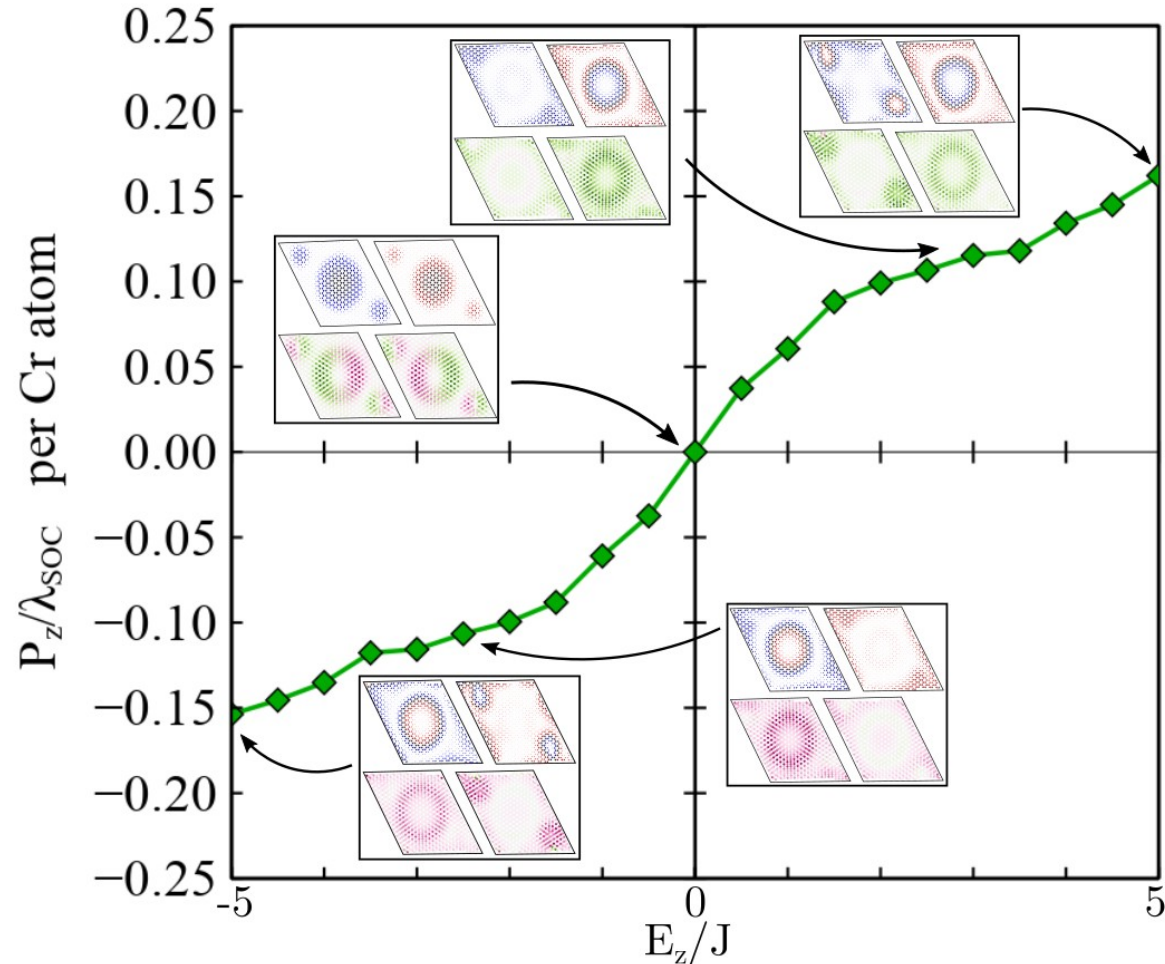
$E/J=3$



Spin Hamiltonian

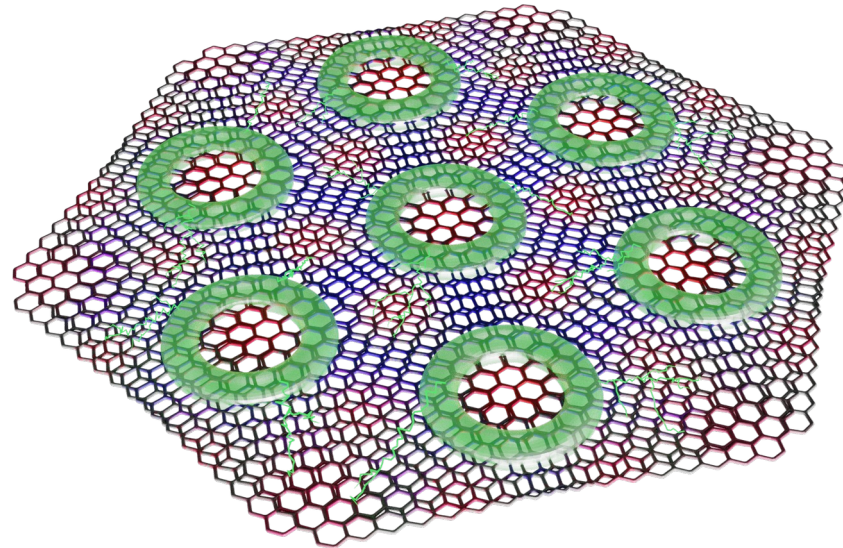
Magnetoelectric Coupling

Transitions between magnetic skyrmion phases as a function of the electric field (1–10 V)



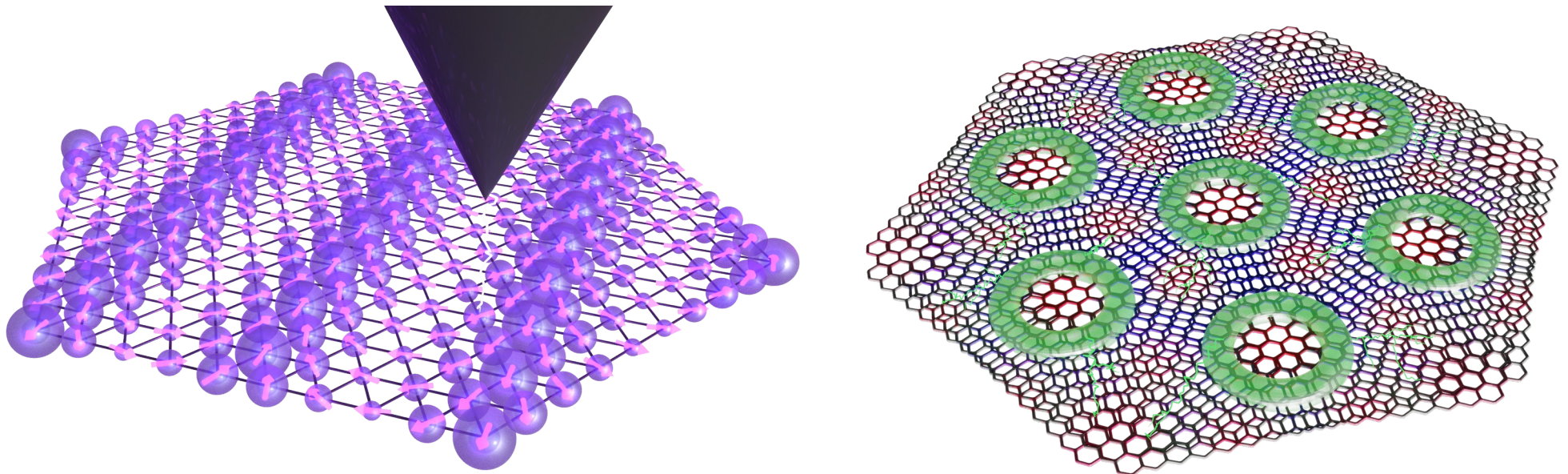
Take home messages

- The strongest Artificial moiré multiferroic order is displayed by twisted CrBr_3 bilayers
- Accessible magnetic skyrmion phases with electric fields



Adolfo O. Fumega and Jose L. Lado, *2D Materials* 10, 025026 (2023)

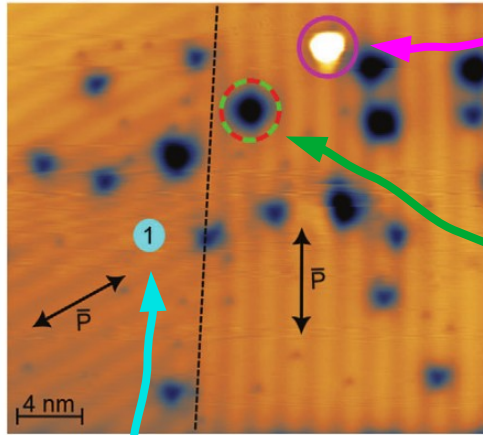
Multiferroic van der Waals Materials are promising for Novel Technological Applications



Back-Up slides

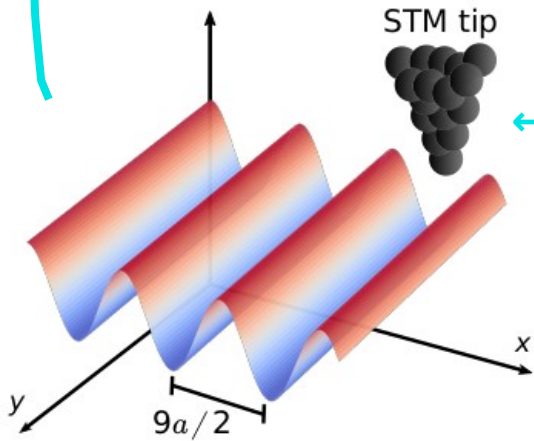
Manipulation of multiferroic domains in monolayer NiI_2

a Height 0 Å 4.5 Å



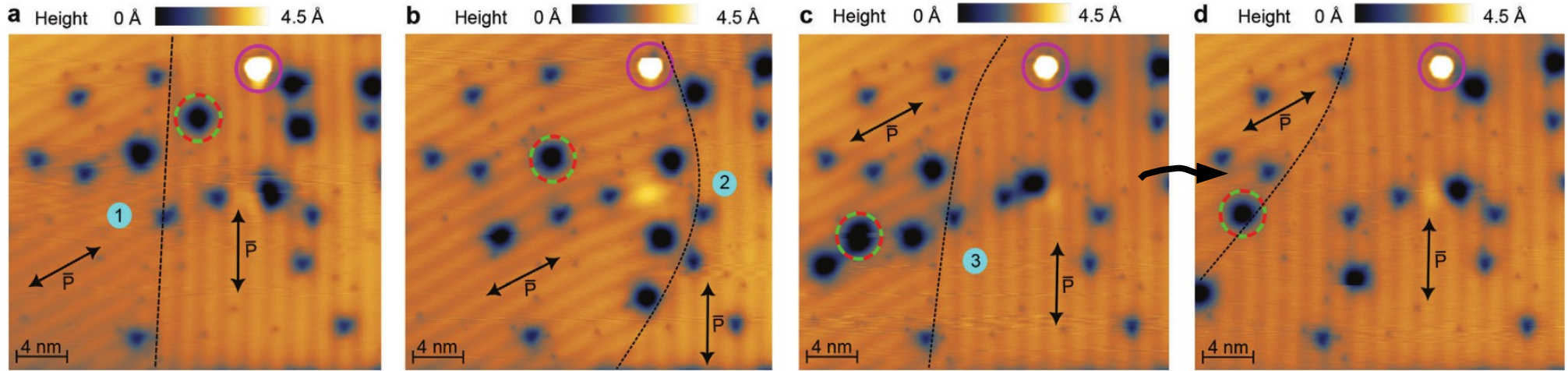
Neutral defect
(used as spatial reference)

Mobile charged defect



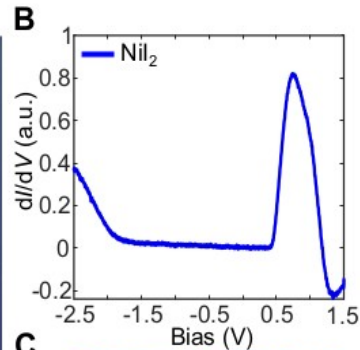
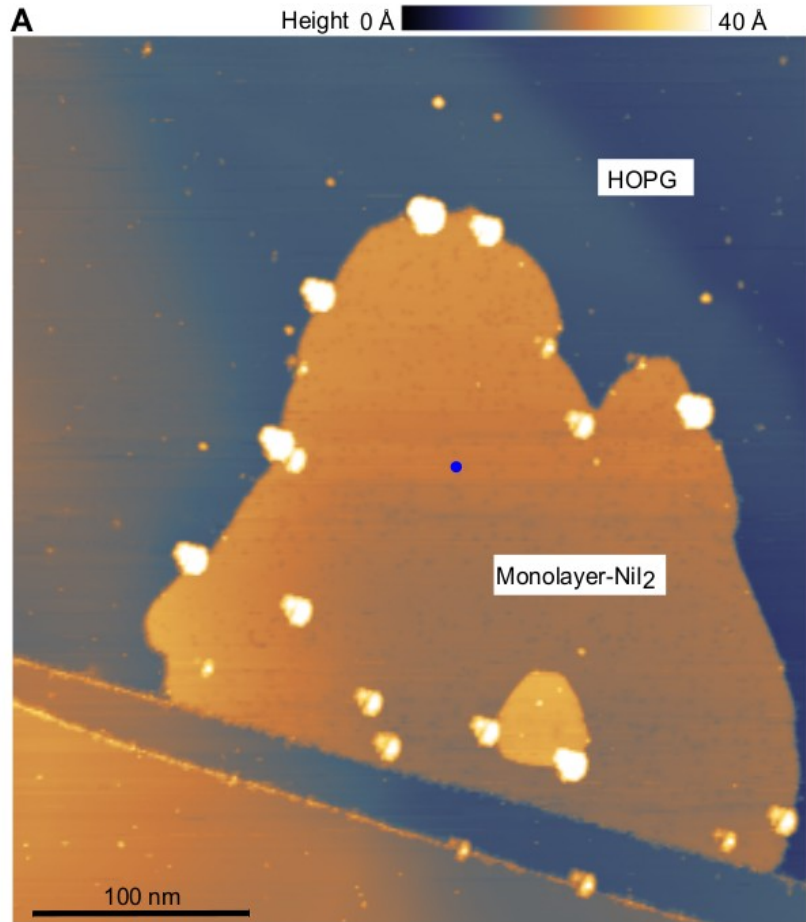
Voltage pulses

Manipulation of multiferroic domains in monolayer NiI_2

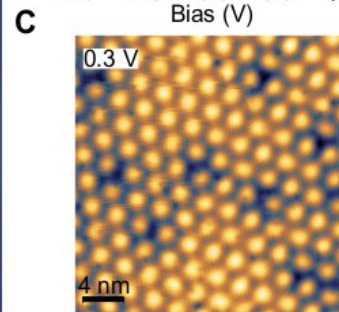


Manipulation of multiferroic domains!

STM characterization of monolayer NiI_2



Monolayer NiI_2 is an insulator with a gap of 2.3 eV (from -1.9 to 0.4 V)

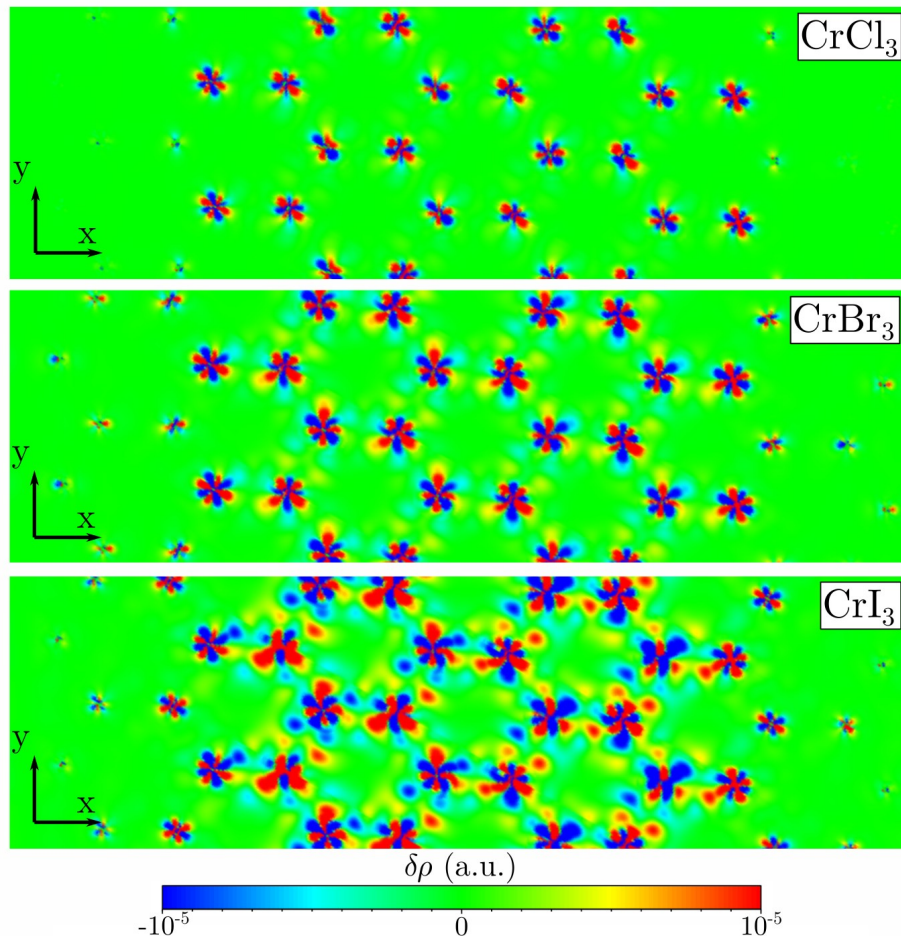


Scan within the gap (HOPG states)

→
Moiré pattern between triangular lattices of NiI_2 and HOPG

Ab initio calculations

Electric polarization in a spin texture of CrX_3



Electronic Density
difference

